Experimental Study on a Continuous HTL Product Separation and Demineralisation System

Esben Ravn
Energy Technology, TEPE4-1002

M.Sc. Thesis

STUDENT REPORT
AALBORG UNIVERSITY

Copyright © Aalborg University 2019

Department of Energy Technology
Aalborg University
http://www.aau.dk

AALBORG UNIVERSITY
STUDENT REPORT

Title:
Experimental Study on a Continuous HTL Product Separation and Demineralisation System

Theme:
M.Sc. Thesis

Project Period:
Spring Semester 2019

Project Group:
TEPE4-1002

Participant(s):
Esben Ravn

Supervisor(s):
Thomas Helmer Pedersen - *Academic*
Lasse Aistrup Rosendahl - *Academic*
Claus Uhrenholt Jensen - *Company contact*

Copies: 1

Page Numbers: 66

Date of Completion:
May 31, 2019

Abstract:

Through this report, the continuous phase separation of HTL products and the demineralisation of HTL oil in the presence of CO_2 as acidification agent are developed. The work was conducted by experimental campaigns on the CSD, which is based on Steeper Energy's proprietary Hydrofaction™ technology. A demineralised oil with an ash content of 0.06 wt.% was achieved, which have never been achieved in the lab-scale batch experiments of the process. The results were not consistent due to the unstable operations of the system. One of the primary instabilities was that the phases shifted position in the separator vessels. This behaviour was studied in batch experiments, where the solubility of CO_2 in the oil and aqueous phase of the process was studied. Based on the batch experiments, CO_2 is 2.4 and 3.5 times more soluble in the oil phase than in RO water. As the density of the liquid phases presumably increases with CO_2 concentrations, this could be the reason for the phase shift.

Publication (with reference) may only be pursued due to agreement with the author - eravn14@student.aau.dk.

Energiteknik
Aalborg Universitet
http://www.aau.dk

AALBORG UNIVERSITET
STUDENTERRAPPORT

Titel:
Eksperimentielt studie af et kontinuertlig HTL-produktseparerings- og demineraliseringssystem

Tema:
Kandidat speciale

Projektperiode:
Forårssemestret 2019

Projektgruppe:
TEPE4-1002

Deltager(e):
Esben Ravn

Vejleder(e):
Thomas Helmer Pedersen - *Akademisk*
Lasse Aistrup Rosendahl - *Akademisk*
Claus Uhrenholt Jensen - *Virksomhedskontakt*

Oplagstal: 1

Sidetal: 66

Afleveringsdato:
31. maj 2019

Abstract:

I denne rapport udvikles den kontinuerlige faseseparation af HTL-produkter og demineraliseringen af HTL-olie ved tilsættelse af CO_2 som forsuringsmiddel. Arbejdet blev udført gennem eksperimenter på det kontinuerlige separations- og demineraliseringssystem, der er baseret på Steeper Energy's proprietære Hydrofaction™ teknologi. En demineraliseret olie med et askeindhold på 0,06 wt.% blev opnået, hvilket aldrig før er opnået i laboratorieforsøg af processen. Resultaterne var ikke konsistente på grund af systemets ustabile drift. En af de primære ustabiliteter var, at faserne skiftede position i separationsbeholderne. Denne opførsel blev undersøgt i batchforsøg, hvor opløseligheden af CO_2 i olie og vandfase af processen blev undersøgt. Baseret på batchforsøgene er CO_2 2,4 og 3,5 gange mere opløselig i oliefasen end i RO-vand. Da densiteten formodentlig øges med koncentrationer af CO_2, kan dette være årsagen til faseskiftet.

Offentliggørelse (med kildeangivelse) må kun ske efter aftale med forfatteren - eravn14@student.aau.dk.

Contents

Preface

This M.Sc. thesis is an experimental study on Steeper Energy's proprietary Hydrofaction™ separation and demineralisation process. The project has been conducted in collaboration with Steeper Energy.

Reading Guide

Figures, equations and tables are numbered according to the chapter of their appearance. For example, the third figure in Chapter 4, will be numbered 4.3, same applies for equations and tables. Every figure and table is provided with a caption, explaining its content.

Nomenclatures describing variables used in equations, will be placed after each set of equations, with a symbol, a description and a unit. When an abbreviation is first introduced in the text, it will be written in full, followed by the abbreviation presented in parenthesis. A separate nomenclature list at the beginning of the report will display a list of the abbreviations used.

Throughout the report, citations appear as numbers in brackets. The numbers will refer to the complete bibliography in the end of the report. Books and articles are listed with author, title, year, and publisher, and websites are listed with author, title, URL and date.

Appendices are placed at the end of the report and are denoted A, B and so on.

Aalborg University, May 31, 2019

Nomenclature

$BPR.\#$ Back Pressure Regulator

CA Citric Acid

$CBS1$ Continuous Bench Scale

$CFPump.\#$ Continuous Flow Pump

CSD Continuous Separation and Demineralisation

EES Engineering Equation Solver

EU European Union

GHG Green House Gas

HTL Hydrothermal Liquefaction

IEA International Energy Agency

$L.\#$ Conductive Level Sensor

MEK Methyl Ethyl Ketone

PFD Process Flow Diagram

$Pressure - 2$ Pressure of the CSD's vessel 2

$Pressure - 3$ Pressure of the CSD's vessel 3

RO Reverse Osmosis

$RO - 2flow$ RO water flow into vessel 2 of the CSD

$RO - 3flow$ RO water flow into vessel 3 of the CSD

$S.\#$ Scale

SDS Sustainable Development Scenario

TAN Total Acid Number

$Temp - 2$ Temperature of the CSD's vessel 2

$Temp - 3$ Temperature of the CSD's vessel 3

$V.\#$ Valve

W/O Water in Oil

$ww2$ Waste water from vessel 2 of the CSD

$ww3$ Waste water from vessel 3 of the CSD

1 Background

On the path towards decarbonisation of the transport sector, no proper solution yet exist for heavy transport (i.e. heavy trucks, marine and aviation). This sector is difficult to electrify, and despite efficiency increases in the sector, the Green House Gas (GHG) emissions keep increasing [6]. Biofuels, and in particularly advanced biofuels can contribute significantly to the decarbonisation of the heavy transport sector in a sustainable manner [7]. Advanced biofuels are produced from non-food biomass wheres conventional biofuels are produced from food crops.

The European Union (EU) focuses on the development of technologies for producing transport biofuels. Member states are committed to reaching 14 % renewables in transport fuels by 2030 [1]. Advanced biofuels are double-counted towards the target of 14 %, which implies that the member states are rewarded for choosing advanced biofuel technologies instead of conventional biofuel technologies. According to the International Energy Agency (IEA), the development of plants for producing advanced biofuels need to be accelerated [11]. In order to meet the Sustainable Development Scenario (SDS) from IEA, the capacity of advanced biofuel-producing plants need to reach 2.3 billion litres by 2023, and the capacity was 0.4 billion litres in 2017 [11]. The capacity of advanced biofuel-producing plants is illustrated in Figure 1.1.

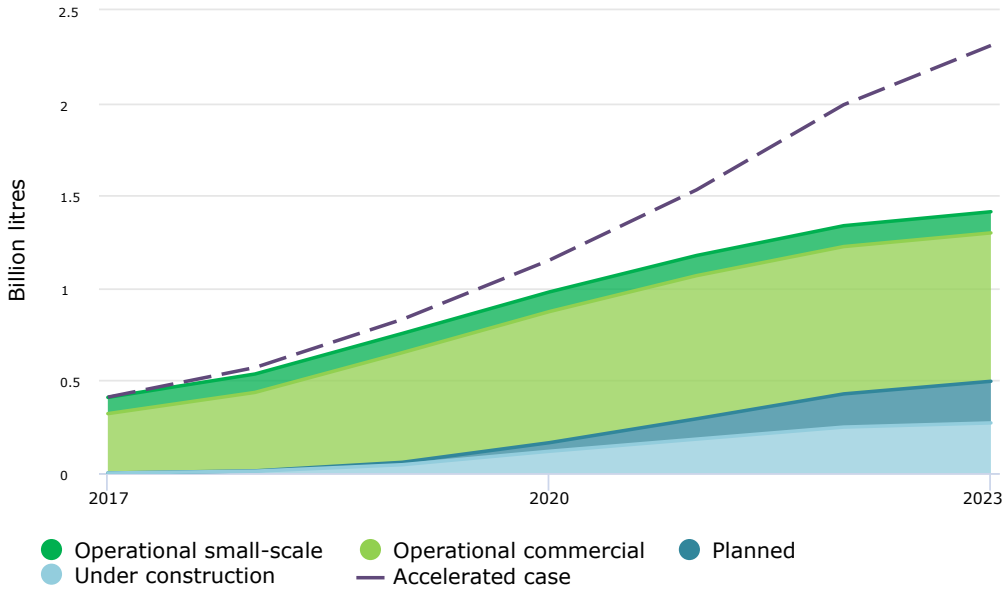

Figure 1.1: Projected and current capacity for advanced biofuel-producing plants. Edited from [11]

In [13] six conversion pathways for renewable jet fuel production are studied. It compares the short-term economic feasibility of the conversion pathways and finds that the Hydrothermal Liquefaction (HTL) is one of the most feasible solutions. Hydrofaction™ , which is Steeper Energy's proprietary HTL technology for efficient conversion of biomass into advanced liquid biofuels, can contribute to a sustainable solution for decarbonisation of the heavy transport sector. The technology fits well into the already existing infrastructure of transportation fuels due to the similarities between Hydrofaction™ biocrude and fossil crudes [12]. In general, biocrudes are oxygenated and need to be deoxygented to meet transport-fuel specifications. In the Hydrofaction™ technology platform the oil is deoxygeneted by hydrotreating. The upgraded biocrude can enter the already established refinery industry, which is one of the advantages with the Hydrofaction™ technology.

The main process streams of the Hydrofaction™ process are illustrated in Figure 1.2. The HTL process and hydrotreating have been proven to run continuously in pilot scale [12]. The product from the HTL process is a mixture of oil, water, gas and inorganics, where the oil needs to be separated from the others before it can be further processed. The separation and demineralisation process is essential as conventional hydrotreating is sensitive to high inorganic and water content of the oil, which can induce fouling and deactivation of the catalyst beds [10]. The separation and demineralisation of the Hydrofaction™ oil have been proven in batch-wise procedures by Steeper Energy and by [12]. Next step is to prove

the technique in a continuous pilot scale. As illustrated in Figure 1.2, the separation and demineralisation process is the link between biocrude production and hydrotreating and is necessary to prove in continuous pilot scale towards a fully continuous Hydrofaction™ process.

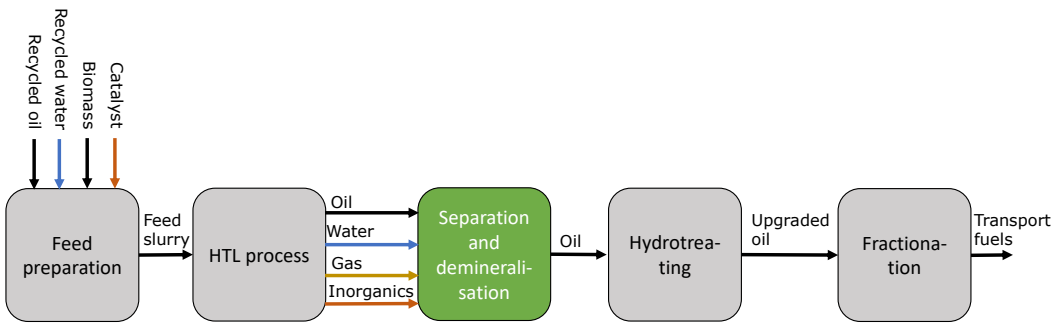

Figure 1.2: The Hydrofaction™ technology main process. Green marks the focus of this project. Note that only the main process flow is illustrated. From the separation of the HTL process products, an oil and aqueous phase are recycled and added in the feed preparation.

In the previous procedure for the separation and demineralisation of the Hydrofaction™ oil, Citric Acid (CA) and rotary evaporators are used with satisfying results; CA for acidification, which improves demineralisation of the oil, and a rotary evaporator for removing water at the end of the process. Inorganic content was reduced from 37000 ppm to 370 ppm, and water content of the oil was reduced from 14.3 wt.% to 0.6 wt.% [12]. This procedure is though time-consuming, and the CA is a consumable, which are two of the motivational reasons for designing and building a new separation and demineralisation system. The new system is continuous, which reduces the time consumption and is a more scalable solution; it utilises CO_2(aq) as acidification agent [14], which is an excess product from the HTL process. This reduces the consumption of consumables in the process.

In [12] CO_2 as the acidification agent was tested in lab scale experiments. Inorganic content of a Hydrofaction™ oil was reduced fromr 42000 ppm to 1019 ppm. This result emphasises that the CO_2 as an acidification agent can demineralise the Hydrofaction™ oil.

One of the success criteria for the separation and demineralisation process is to get below 15 ppm inorganic content in the oil, which would result in a hydrotreatable oil in terms of inorganics content. The value is given by Steeper Energy.

1.1 The CBS1

The Continuous Bench Scale Hydrofaction™ Plant 1 (CBS1) is the pilot plant at which the Hydrofaction™ technology is being developed and demonstrated. The pilot is a product of the collaboration between Aalborg University, which owns the plant, and Steeper Energy, which operates the plant. It has >1750 oil-producing operating hours, and in Q3-Q4 2018 its feed preparation and separation and demineralisation system were upgraded from semi-batch to a continuous operating principle. The Process Flow Diagram (PFD) of the CBS1 is illustrated in Figure 1.3. The pilot plant is located at Aalborg University and is build inside the containers, depicted in Figure 1.4.

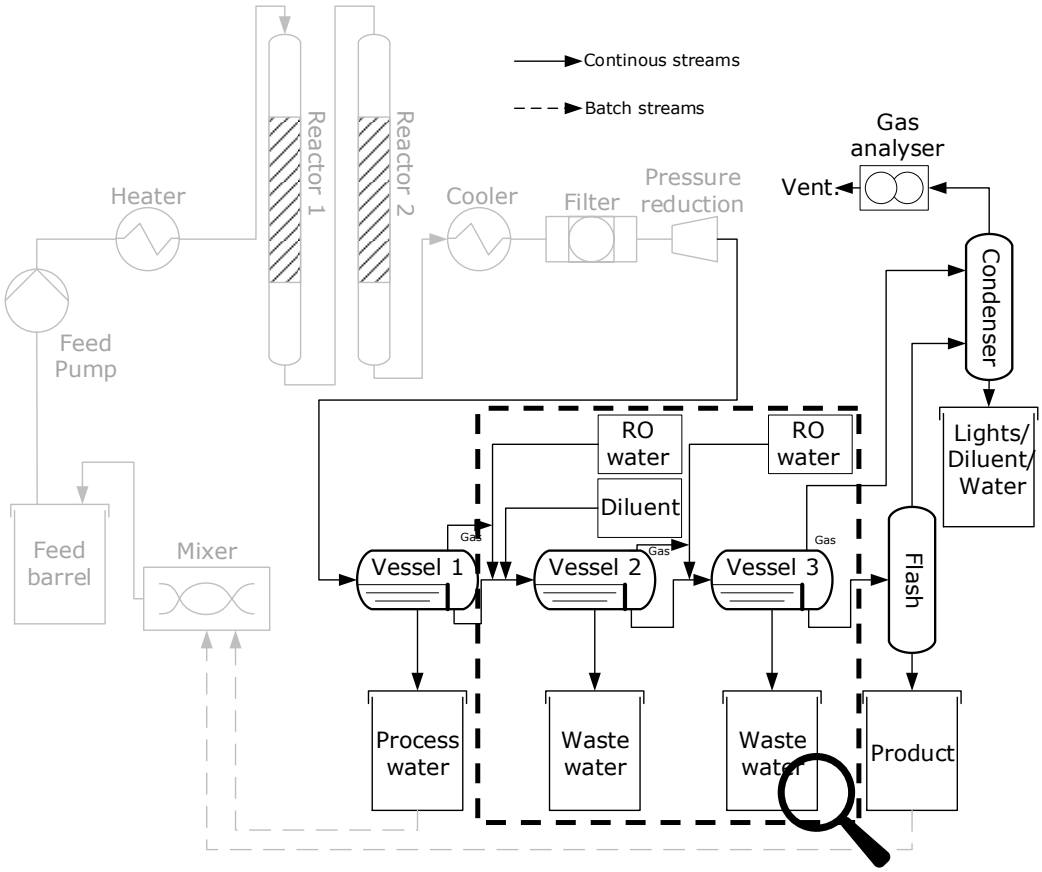

Figure 1.3: Simplified PFD of the CBS1. The non-transparent components and lines represent the pilot's separation and demineralisation system. The magnifying glass illustrates the experimental focus of this project. RO is the abbreviation for Reverse Osmosis. Edited from [12].

Figure 1.4: Picture of the pilot plant.

1.2 The CSD

The continuous separation and demineralisation system of the CBS1, referred to as the CSD, is a new state-of-the-art system. Its main functions are to reduce inorganic and water content of the Hydrofaction™ oil and separate the three phases entering the system from each other; An aqueous phase, an oil phase and a gas phase. Going from a lab scale proof of concept to a continuous pilot scale naturally increases the complexity of the system. However, it is hypothesised that by experimental testing on the pilot-scale CSD, one would achieve more relevant knowledge about the separation and demineralisation process for a commercial scale system, than if the process is further tested by lab-scale experiments. It is also in the interest of Steeper Energy to prove the principle of the CSD towards commercialisation of the Hydrofaction™ technology platform. A detailed version of the CSD is illustrated in Figure 1.5.

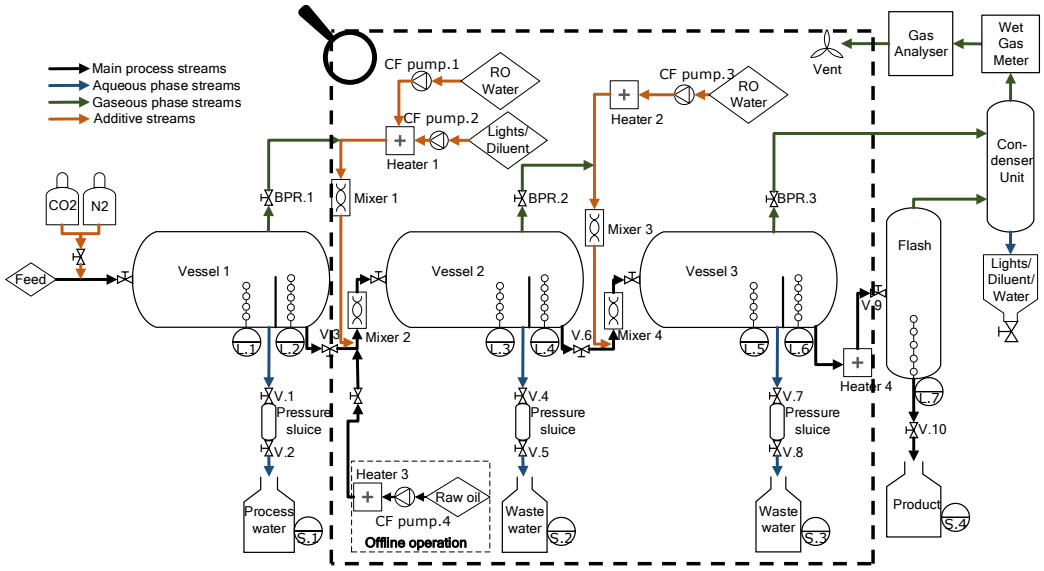

Figure 1.5: PFD of the CSD. It is a simplified version of the original PFD. However, relevant components for this project are displayed in this figure. As in Figure 1.3 the experimental focus of this project is marked by the magnifying glass.

- **Vessel 1:** Process flow from the oil-producing part of the CBS1 enters vessel 1, where the process aqueous phase is extracted and recycled in the Hydrofaction™ process. The oil phase is partially demineralised and led into vessel 2. The gaseous phase is led through each vessel and in the end to the ventilation.

- **Vessel 2:** Aqueous CO_2 is the acidification agent of the CSD - RO water is thereby mixed with the process gas prior to entering vessel 2. The diluent is added to dilute the oil phase from vessel 1 to reach a sufficiently low density, such as the oil phase floats on top of the aqueous phase. The oil phase is further demineralised, and it is expected that in vessel 2 the highest demineralisation rate is achieved. The aqueous phase, which is separated from the oil phase, is extracted and is a waste product of the process.

- **Vessel 3:** The process gas is mixed with RO water to acidify the environment. The carbonated water is mixed with the oil phase prior to entering vessel 3, where the aim is to reach an inorganic content sufficiently low to make the oil upgradable/hydrotreatable.

- **Flash vessel:** The diluent, and the remaining water of the oil phase is flashed off in the flash vessel.

- **Online/offline operation:** The CSD can be operated in online and offline mode, where online is when the whole CBS1 is in operation, and offline is when only the CSD is in operation. In offline operation mode vessel 1, is not in operation and feed is pumped directly into vessel 2.
- **Automatic control of liquid flows:** Liquid flows within the system are controlled automatically by conductive level sensors (L.1 to L.7). These sensors detect the interfaces between the phases in the separator vessels due to the difference in conductivity of the phases. They control the liquid flows by needle valves (V.3, V.6, V.9, and V.10 in Figure 1.5) for the oil phase and sluice systems for the aqueous phase.
- **Temperature and pressure:** The separator vessels are pressurised to increase the amount of CO_2. The system is approved up to 50 bar. The CSD is monitored by temperature and pressure sensors mounted inside the separator vessels and lines between the vessels.
- **Mass balances:** Scales, a wet gas meter (measuring the volumetric flow of gas), and a gas analyser, enables the operator to calculate mass balances.

The PFD of the CSD in Figure 1.5 is rather complex and in order to illustrate the adjustable operating conditions of the CSD, Figure 1.6 is presented. The outputs of interest are the inorganic and water content in the oil, as these values are a measure of how well the CSD performs.

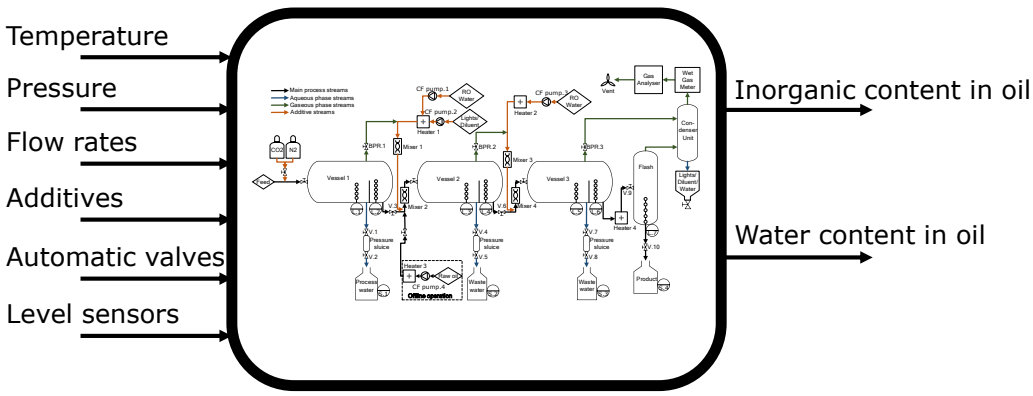

Figure 1.6: Illustration of input parameters (adjustable operating conditions) for the CSD and its outputs of interest. The input parameters can be adjusted in several parts of the CSD. E.g., temperature is adjustable by four heaters and by nine sections of heat tracing. This adds up to the complexity.

In summary, the CSD is a complex system with a large number of adjustable parameters. It is considerably more complex than the lab-scale batch reactors, where the previous development of the process have been conducted.

1.3 The Three-Phase Separator Vessels

The design of the three-phase separator vessels, named vessel 1, 2 and 3 in Figure 1.3, is illustrated in Figure 1.7. Solids and inorganic content of the oil phase precipitate during the separation and demineralisation process. It is preferable that the content settles in the aqueous phase, as this is, in most cases, the waste product of the process. The three-phase separator vessels are designed such that the aqueous phase is the bottom phase, the oil phase is in the middle, and the gas phase is the top. The oil phase is led above an overflow plate and through its outlet.

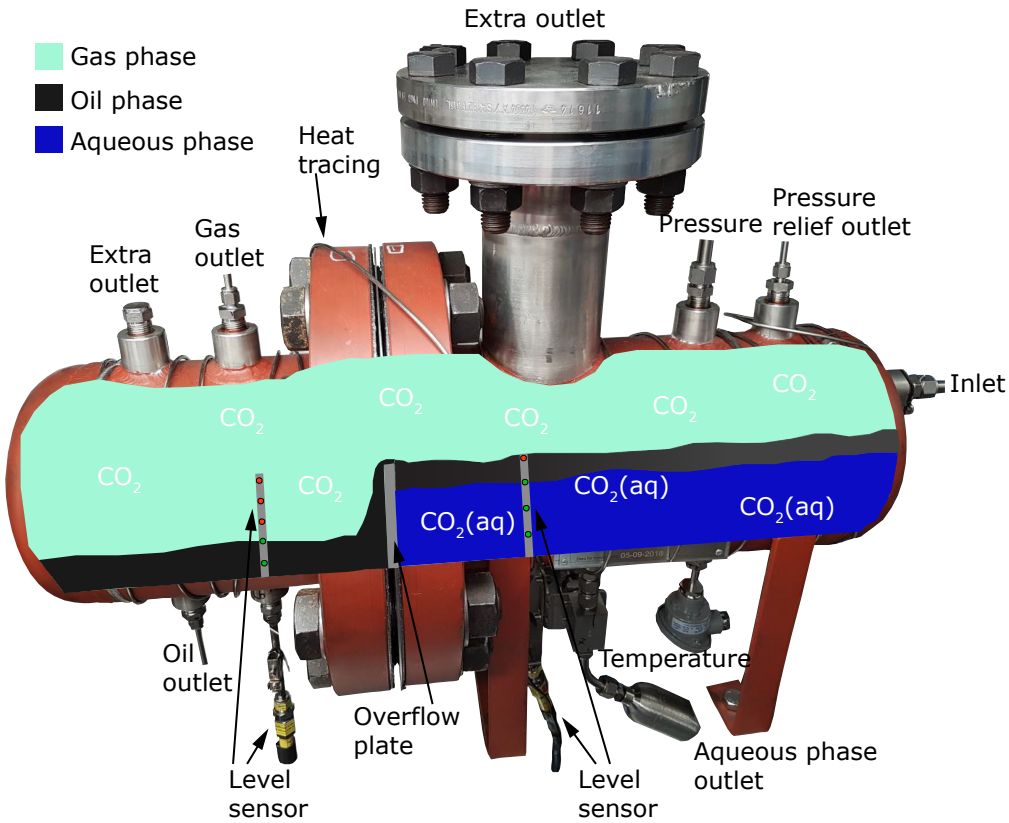

Figure 1.7: Illustration of the three-phase separator vessels. The green dots on the level sensor illustrates detectable conductivities and the red dots illustrates undetectable conductivities. Note that the vessel is mirrored if compared to the separator vessels in Figure 1.3.

Vessel 1 of the CSD, which separates the HTL process products from each other, has partly been commissioned in [22]. Experimental studies on the commissioning of vessel 2 and 3 are this project's focus, as the vessels have not yet been commissioned and further development of this part of the process in order to scale up the technology.

2 Problem Statement

In this chapter, the overall objective of the report is presented together with its working questions. The structure of the report is also presented.

The main objective of this project is to improve the understanding of the continuous separation and demineralisation process for the Hydrofaction™ technology. The process utilises CO_2(aq) as an acidification agent, which has been proven in [12] by lab-scale batch experiments to demineralise the oil.

By experimental studies on the newly build CSD, the knowledge platform can be extended further by the additional complexity of a continuous system compared to lab-scale batch reactors. The studies are performed on vessel 2 and 3 as this is the next step in the commissioning of the CSD. The main objective is formulated in the following problem statement and working questions.

Problem statement:

- **What parameters influence the separation of HTL products and the demineralisation of HTL oil when using CO2 as an acidifying agent in the continuous CSD?**

Working questions:

- How does operating conditions in general and in the CSD affect the separation and demineralisation process?
- How can the results from the commissioning tests be interpreted, in order to further develop the separation and demineralisation process?

2.1 Report Structure

In Figure 2.1, the structure of the report is illustrated as a flow chart. First, the separation and demineralisation technique with CO_2 as acidification agent is discussed. Secondly, the commissioning experiments are presented, and results are discussed. Thirdly, simpler experiments, which are experiments designed to achieve knowledge about the process, are presented, and its results are discussed. Based on the three steps, the further development of the separation and demineralisation process of the Hydrofaction™ technology platform are discussed.

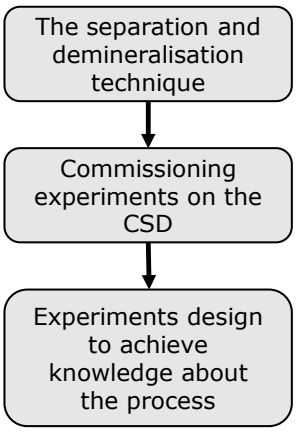

Figure 2.1: Structure of the report

3 Separation and Demineralisation of HTL oil in the Presence of CO_2

In this chapter, the theoretical background for the Hydrofaction™ separation and demineralisation process is established. Firstly, the three phases of the Hydrofaction™ product are described, and secondly, the relevant and important features of the separation and demineralisation process are studied.

3.1 The Three Phases

Three phases are present in an HTL derived product - an oil, an aqueous, and a gas phase. Additionally, inorganics are potentially dissolved in the two liquid phases. In the Hydrofaction™ technology, the separation of the three HTL phases and the demineralisation of the oil phase are controlled by various parameters, such as temperature, pressure, flow rates and additives. It is essential to study the different parameters and their impact on the process. However, prior to understanding the separation and demineralisation process, the three phases need to be studied and characterised.

3.1.1 The Oil Phase

The Hydrofaction™ oil phase is a water in oil (W/O) emulsion, which typically contains 1-5 wt.% inorganics and 6-20 wt.% water. These values are obtained during the commissioning tests on vessel 1 of the CSD. A Hydrofaction™ oil emulsion is depicted in Figure 3.1. The inorganic content is primarily potassium and sodium, as this is added in the feed preparation as a homogeneous catalyst, potassium carbonate (K_2CO_3), and a pH adjustment agent, sodium hydroxide (NaOH), [12]. In the separation and demineralisation process, the aim is to destabilise the oil emulsion to reduce inorganic and water content of the oil phase. The destabilisation can be rather tricky, as some of the oil compounds stabilise the emulsion. The oil emulsion is stabilised by, among others, compounds with an amphiphilic nature,

solids with melting points well above ambient, which could trap water droplets in the solids, and oxygen levels. On a dry ash free basis, the Hydrofaction™ oil contains around 10 wt.% oxygen [12], which makes the oil more polar than fossil crudes and by that, it has a stronger affinity to water.

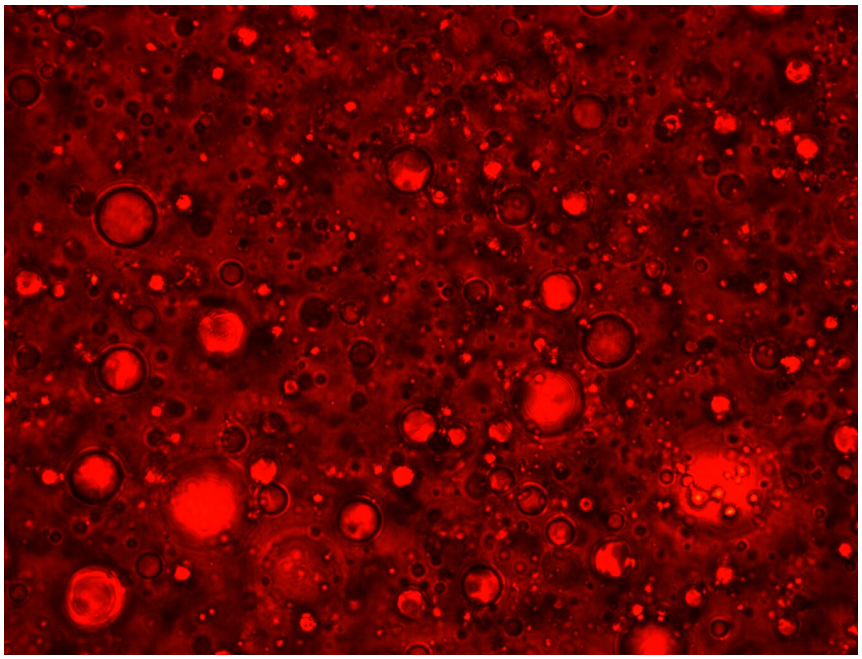

Figure 3.1: Transferring light optical microscopy (100x) of a Hydrofaction™ oil emulsion [12].

As given in [12], the Total Acid Number (TAN) of the dehydrated and demineralised Hydrofaction™ oil is around 50 mgKOH/g, which is approximately an order of magnitude higher than a 'high TAN' fossil crude. TAN is the mass of KOH in milligrams, which is required to neutralise 1 g of a substance and is a measure of the amount of acid groups in the substance [19], which could be carboxylic acid groups. These acid groups can together with an alkali metal, e.g. Na^+ and K^+, form caboxylates. This reaction is presented in Equation 3.1 with sodium hydroxide as an example. The oil emulsion is stabilised by the formation of carboxylates, due to their amphiphilic nature.

$$\mathrm{NaOH} + \mathrm{RCOOH} \rightarrow (\mathrm{RCOO})\mathrm{Na} + \mathrm{H_2O} \tag{3.1}$$

The detachment of the inorganic content in the oil emulsion can be achieved by acidification as this protonates the carboxylic acid groups and releases the inorganic content. The detachment reaction possibly occurs as in Equation 3.2, with sodium as an example and CO_2(aq) as the acidification agent.

$$(\mathrm{RCOO})\mathrm{Na} + \mathrm{CO_2(aq)} + \mathrm{H_2O} \rightarrow \mathrm{RCOOH} + \mathrm{Na(HCO_3)} \tag{3.2}$$

It is interesting to study the assumption about carboxylic acid groups and carboxylates in the Hydrofaction™ oil, because another hypothesis is that the measured inorganic content in the oil (1-5 wt.%) could also be inorganics dissolved in the water content of the oil emulsion. If all inorganic content is situated in the oil part of the emulsion and is forming carboxylates, the inorganic capacity of the oil can be estimated by examining the TAN. The analysis of the TAN can indicate if it is reasonable to consider some of the inorganics to be situated in the oil of the emulsion.

For a dehydrated and demineralised Hydrofaction™ oil, the TAN is measured to be between 45 and 67 [12]. For an oil, before separation and demineralisation, the TAN is measured to be 8 [12]. If these TAN values are considered valid in general for the oil, the inorganic capacity of the oil can be estimated. For the estimation, the TAN values are considered to be the measure of the amount of carboxylic acid groups in the oil and all inorganic atoms are attached to its own carboxylic acid group. The postulate is that every K^+ (from the measurement of the TAN) dissolved in the oil is attached to the conjugate base of a carboxylic acid group. By comparing the molar weight of K^+ to KOH, which is 0.70, the inorganic capacity of the oil is estimated.

$$\begin{aligned} Inorganic_{capacity} =& (45-8)\ to\ (67-8) mg\mathrm{KOH}/g \cdot \frac{MW_{\mathrm{K^+}}}{MW_{\mathrm{KOH}}} && (3.3) \\ =& 37\ to\ 59 mg\mathrm{KOH}/g \cdot 0.70 = 26\ to\ 41 mg\mathrm{K^+}/g && (3.4) \end{aligned}$$

From Equation 3.4 the amount of K^+ in Hydrofaction oil is between 2.6 and 4.1 wt.%. If all the inorganic content behaves as K^+, the inorganic capacity of the oil is between 2.6 and 4.1 wt.%, which is in the range of the measured 1-5 wt.%. From the inorganic capacity estimation, it is possible that inorganics are located in the oil of the emulsion. However, it is also suspected that inorganics are dissolved in the water of the emulsion due to their solubilities in water. Inorganic content of the process water (the aqueous phase, which is entering vessel 1 of the CSD) is measured to approximately 10 wt.% for CBS1 runs in Q1 2019. If the water content of the emulsion is 6-20 wt.% and is process water with 10 wt.% inorganics, 0.6-2 wt.% of the inorganic content of the emulsion is situated in the water. Based on

the above analysis on the inorganic content of the emulsion, it is expected that inorganic content is both situated in the oil and water content of the emulsion.

To understand the separation between the water and oil in the oil emulsion, the Stokes equation is presented in Equation 3.5. Stokes equation can only model a simplified version of the separation between the aqueous solution and the oil of the emulsion by including gravitational and viscous forces. The equation does not include the behaviour of the amphiphilic surfactants, the solid oil compounds etc.

$$v = \frac{2r^2 \Delta\rho g}{9\mu} \tag{3.5}$$

- v is the sedimentation speed of the dispersed droplets [m/s].
- r is the droplet radius [m].
- $\Delta\rho$ is the density difference between the continuous and dispersed phase [kg/m^3].
- g is the gravitational acceleration [m/s^2].
- μ is the viscosity of the continuous phase [Pa·s].

A higher density between the water and oil increases the sedimentation speed of the water droplets, which may be achieved by increasing temperatures. Higher temperatures also lower the viscosity of the oil, which increases the sedimentation speed as well.

3.1.2 The Aqueous Phase

In the separation and demineralisation process, the aim is to separate the aqueous phases from the oil phase, which can be achieved by increasing the density difference between phases and extracting them through individual outlets - like the depicted three-phase separator in the CSD Figure 1.7.

The pH value of the aqueous phase could be used as a measure of how well the oil is demineralised. The definition of pH is presented in Equation 3.6 and is a measure of the concentration of free protons, H^+, in a substance.

$$pH = -log([\mathrm{H}^+]) \tag{3.6}$$

The pH value decreases (= higher concentration of H^+) as the environment of phases is acidified. As the carboxylic acid groups are protonated the pH value increases due to the usage of H^+. By measuring the pH value of the aqueous phase it may be possible to assess the demineralisation performance; A higher pH value could imply a higher usage of H^+ and thereby a better demineralisation of the oil. However, samples of the aqueous phase are taken at ambient pressure, and most of the CO_2 dissolved in the aqueous phase eventually escapes into the air. This causes uncertainties in the relation between the pH of the aqueous phase and the demineralisation performance of the oil.

3.1.3 The Gas Phase

In the Hydrofaction™ process, biomass is both converted into oil compounds and gaseous compounds. The composition of the gas is continuously monitored in the CBS1, as illustrated by the gas analyser in Figure 1.3. From online operations on the CBS1 in Q1 2019, the composition of the gas phase has been measured to be:

- $\approx$ 80 vol.% CO_2.
- $\approx$ 15 vol.% H_2.
- $\approx$ 5 vol.% CH_4.
- $\approx$ 0.2 vol.% CO.

The high concentration of CO_2 is desirable due to its ability to acidify the environment by reacting with water. CO_2 is also soluble in the oil phase, which could cause complications in terms of a lower concentration of CO_2 in water and changing properties of the oil phase, leading to a need for understanding the phase equilibria of the system.

In the experimental study a gas phase of 100 vol.% CO_2 is used, as the experiments are performed in offline operation mode. In the commissioning of vessel 1 of the CSD in [22], the online process gas is used. The difference in gas composition for the online and offline operation could affect the separation and demineralisation process as CH_4, H_2, and CO are soluble in water and presumably in the oil phase. In Table 3.1, the solubility of the gas components in water are presented.

	CO_2	H_2	CH_4	CO
Solublity [moleGas/moleWater]	$6.1 \cdot 10^{-4}$	$1.7 \cdot 10^{-5}$	$1.4 \cdot 10^{-5}$	$2.6 \cdot 10^{-5}$

Table 3.1: Solubility of process gas compounds in water at 25 °C and 1 atm [17].

From Table 3.1, the solubility of CO_2 in water at 25 °C and 1 atm is around one order of magnitude higher than the solubility of the other compounds in water. The solubility of other gaseous compounds than CO_2 are not studied in this project.

3.2 The Separation of the Three Phases

The Hydrofaction™ oil is an extra heavy oil (>1000 kg/m^3) when compared to fossil crudes [21]. The density of a Hydrofaction™ oil is measured at three different temperatures. These densities are presented in Figure 3.2, together with the density of water.

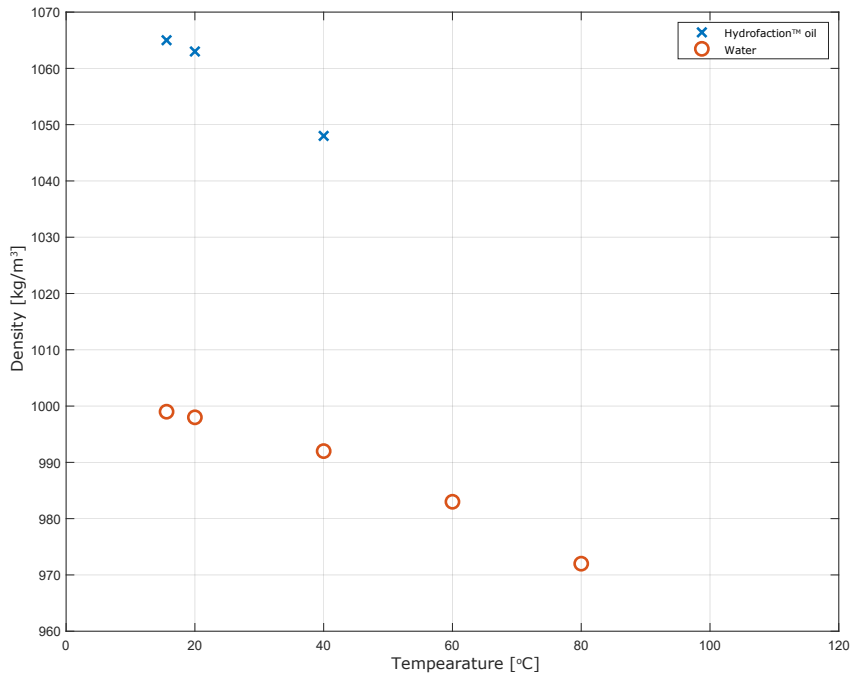

Figure 3.2: Density of a Hydrofaction™ oil and water at different temperatures and 1 bar.

From Figure 3.2, it can be observed that the Hydrofaction™ oil has a higher density than pure water, which potentially complicates the separation and demineralisation process.

In the first separation and demineralisation stage, the aqueous phase is the process water of the Hydrofaction™ products, which has been observed to have a higher density than pure water, due to the dissolved salts. The process water also has a higher density than the oil phase in stage one and thus, the oil phase is floating on top of the process water in the first stage.

In the other separation and demineralisation stages, the oil is washed with RO water, and the density of RO water can be considered similar to the presented density of water in Figure 3.2, as this is for pure water. To separate the aqueous phase and the oil phase in stage two and upstream, the density of the oil phase need to be lowered, which can be achieved by mixing the oil with a diluent.

3.2.1 The Diluent: Methyl Ethyl Ketone (MEK)

As given in [12] MEK is a satisfying diluent for the Hydrofaction™ oil, and other diluents are not considered for this project.

MEK has a density of 805 kg/m^3 at 20 °C [25] and can dilute the Hydrofaction™ oil sufficiently to a lower density than the density of RO water. However, MEK is soluble in water as well, which could lower the density of the aqueous phase and potentially cause separation issues. In [2], the solubility of MEK in water is studied at different temperatures and pressures. Some of the experimental data are presented in Figure 3.3.

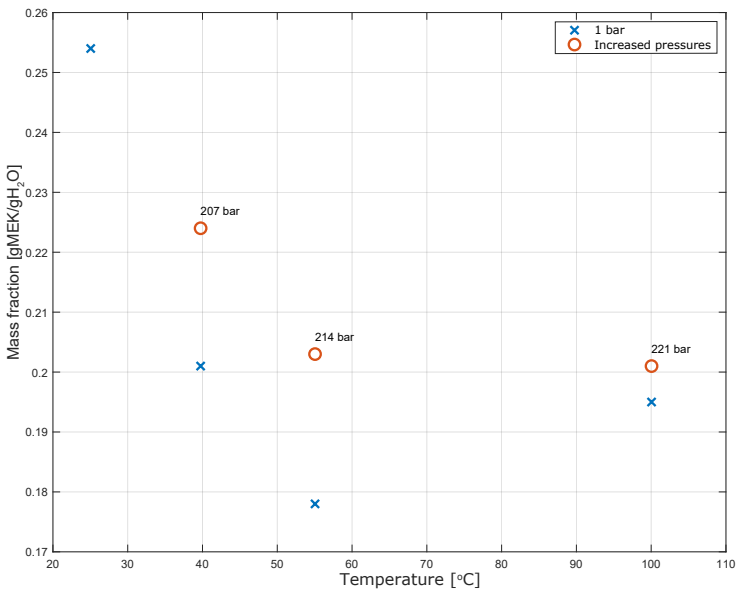

Figure 3.3: Mass fraction of MEK in water [2].

From Figure 3.3, the solubility of MEK in water decreases with temperature between 25 °C and 55 °C. For temperatures above 40, °C the solubility slightly increases with pressure when compared to 1 bar measurements. As the maximum allowed pressure for the CSD is 50 bar, the experimental data from [2] are presented to get an insight of the MEK solubility with respect to pressure. It is not believed that the pressure would affect the solubility considerably in the CSD pressure range. Increasing temperatures could have a positive effect on the separation and demineralisation process in regard to the solubility of MEK in water. Reducing the concentration of MEK in water would result in more MEK remain in the oil phase, and the density difference between the oil and aqueous phase remains sufficient.

3.3 Demineralisation of the Hydrofaction™ Oil

It is proven in [12] that lowering the pH value of the Hydrofaction™ products with citric acid or CO_2(aq) improve demineralisation. CO_2 is the preferable solution, as the process gas consist of a high CO_2 concentration and after the demineralisation process the CO_2 is relatively easy to separate from the product.

3.3.1 Acidification by CO_2

CO_2 is soluble in water where approximately 99 % exists as CO_2(aq) and approximately 1 % exists as carbonic acid, H_2CO_3, which can dissociate to H^+, $HCO_3{}^-$ and $CO_3{}^{2-}$[15], and by that, acidifies the aqueous phase as protons are released. The reaction mechanism for CO_2 in water is presented in Equation 3.7 to 3.9

$$CO_2(aq) + H_2O \rightleftharpoons H_2CO_3 \tag{3.7}$$

$$H_2CO_3 \rightleftharpoons H^+ + HCO_3{}^- \tag{3.8}$$

$$HCO_3{}^- \rightleftharpoons H^+ + CO_3{}^{2-} \tag{3.9}$$

It is hypothesised that the higher the proton concentration is (= lower pH), the more carboxylate salts are protonated and the demineralisation is improved.

In a pure CO_2 + water system, the pH value decreases as function of CO_2 pressure. As CO_2 pressure increases, the pH value decreases and is nearly constant at a value of 3 when 50 bar CO_2 is reached [4, 3]. This is due to equilibrium behaviour and that the reactions are reversible.

The equilibrium constants are dependent on temperatures, which can be estimated by the Van't Hoff equation, presented in Equation 3.10. In Van't Hoff equation the enthalpy of reaction (ΔH_r) is assumed constant.

$$ln\left(\frac{K_{e2}}{K_{e1}}\right) = -\frac{\Delta H_r}{R_{univ}} \cdot \left(\frac{1}{T_2} - \frac{1}{T_1}\right) \tag{3.10}$$

Where:

- $K_{e1,e2}$ is the equilibrium constant at the given temperature, respectively [-].
- ΔH_r is the enthalpy of reaction for the given reaction ($\sum \Delta H_{f,products}$ - $\sum \Delta H_{f,reactants}$) [J/mol].
  - $\Delta H_{f,products}$ is the enthalpy of formation for the products [J/mol].
  - $\Delta H_{f,reactants}$ is the enthalpy of formation for the reactants [J/mol].
- R_{univ} is the universial gas constant, which is 8.314 J/(K · mol).
- $T_{1,2}$ is the temperature associated with the equlibrium constant, $K_{e1,e2}$, respectively [K].

The equilibrium constants for the reactions in Reaction 3.7 and 3.8 are combined, as only ≈ 1 % of the dissolved CO_2 dissociate to H_2CO_3. At standard conditions (25 °C and 1 bar) the equilibrium constant for Reaction 3.7 and 3.8 is $4.45 \cdot 10^{-7}$ and for Reaction 3.9 the constant is $4.69 \cdot 10^{-11}$ [5]. The equilibrium constants can be estimated at different temperatures by Equation 3.10. The equilibrium of each molecule associated with the CO_2 in water reaction mechanism is illustrated in Figure 3.4 as a function of pH. Equilibrium constant calculations are presented in Appendix A.

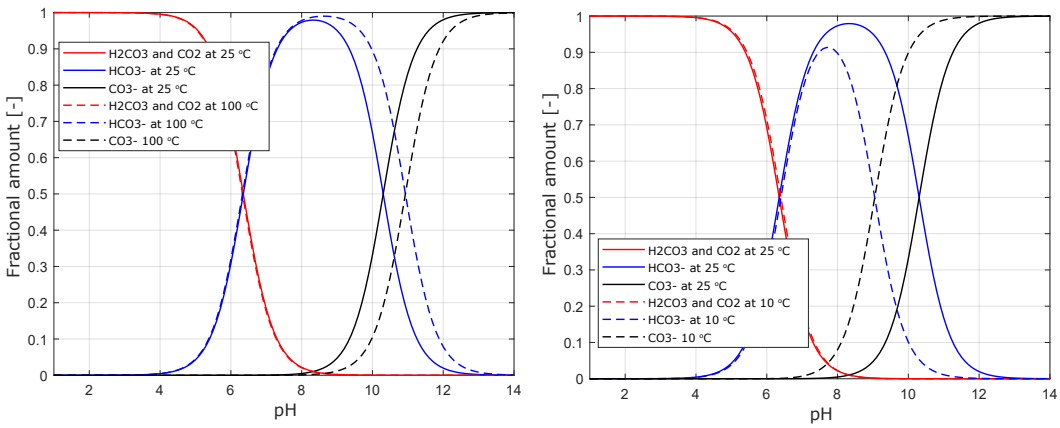

Figure 3.4: Equilibrium of molecules associated with CO_2 dissolved in water as function of pH at 1 bar and 10, 25 and 100 °C.

As illustrated in Figure 3.4, as the pH value decreases and thereby the proton concentration increases, the equilibrium shifts towards H_2CO_3 and CO_2. Above the pH value of 7 the HCO_3^- and CO_3^{2-} fractions are highly dependent on temperatures and unremarkable dependent on temperatures below pH value 7. Temperatures have a little effect on the fraction of the combined H_2CO_3 and CO_2. From Figure 3.4, it is not possible to lower the pH value below ≈ 4 by increasing or lowering the temperature at 1 bar with only CO_2 as acidification agent.

In summary, the pH value can be lowered to a pH value of approximately 3 by increasing the CO_2 pressure. Lower pH values with CO_2 as acidification agent cannot be achieved based on the analysis in this section. Even if a CA solution lowers the pH value of the environment to e.g. a value of 4 before the acidification with CO_2(aq), the pH value would not get below 3 [3].

3.4 Solubility of CO_2 in the Liquid Phases

As CO_2 is dissolved in the different liquid phases, properties of these phases changes, such as density, which is an important parameter for the separation process. Three main liquids are present in the separation and demineralisation process; the aqueous phase, the oil emulsion and the diluent (MEK). The solubility of CO_2 in these liquids can be described by Henry's law, which is presented in Equation 3.11

$$c_{CO_2} = \frac{P_{CO_2}}{K_h} \tag{3.11}$$

Where:

- K_h is Henry's constant [Pa].
- P_{CO_2} is the partial pressure of CO_2 [Pa].
- c_{CO_2} is the CO_2 in liquid mole fraction [-].

According to Henry's law, the higher partial pressure of the gas the higher is the concentration of the gas in the liquid. On the other hand, a higher Henry's constant results in a lower concentration. Henry's constant is dependent on the gas, solvent, and temperature. Typically, a higher temperature results in a lower concentration, due to the increased kinetics of the gas. In the separation and demineralisation process, the partial pressure of CO_2 is considered constant for all liquids, and the solubility of CO_2 in the liquids can then be described only by Henry's constant.

	Henry's constant [bar]			
	15 °C	**25 °C**	**35 °C**	**45 °C**
CO_2 in pure water	1284	1724	2178	2634
CO_2 in brine (5g NaCl/L H_2O)	4065	4878	5882	6897
CO_2 in MEK	50	61	72	82

Table 3.2: Henry's constant at different temperatures for CO_2 in water [16], in brine [8], and in MEK [26].

From Table 3.2 and Henry's law, the solubility of CO_2 in MEK is considerably higher than the solubility of CO_2 in water and especially in a 5 N NaCl aqueous solution. Note that the brine is a NaCl brine and the dissolved salts in the Hydrofaction™ aqueous phase are primarily NaOH and K_2CO_3. However, the different brines are considered comparable and the increase in the Henry's constant for a 5 N NaCl brine vs pure water is considered somewhat valid for the Hydrofaction™ aqueous phase. In the separation and demineralisation process, this is not desired, as the acidification reactions occur together with water and not MEK, It is believed that the higher the concentration of CO_2 is in the aqueous phase, the better is the demineralisation. There is no data on the Henry's constant for Hydrofaction™ oil, however, by experiments later in the report the solubility of CO_2 in all the liquid phases are studied.

3.5 Density of the Liquid Phases vs CO_2 Concentration

From the analysis of the solubility of CO_2 in the liquid phases, it is essential to study the density changes of the liquid phases as a function of CO_2 concentration.

3.5.1 Brine vs CO_2 Concentration

It is preferable that the density of the aqueous phase increases as salts and CO_2 are dissolved in it. This would improve the separation as the aqueous phase is more likely to become the bottom phase in the vessels. In [9] the density of a 2 molNaCl/kgH_2O aqueous solution is studied at 65 °C and 50 bar CO_2 pressure. The density increases from 1055 to 1057 kg/m^3 between the CO_2 unsaturated and saturated brine, which is rather insignificant. The dissolved salts have a greater effect on the density of the aqueous phase, which is approximately 70 kg/m^3 when comparing the 2 molNaCl/kgH_2O aqueous solution with pure water.

3.5.2 Oil Phase vs CO_2 Concentration

No data exist on the density of the Hydrofaction™ oil as a function of CO_2 concentrations and to assess its density change other bio-oils and hydrocarbons are studied.

In [20] the density of rapeseed oil is studied as a function of CO_2 pressures and temperatures at 60 °C and 80 °C. From the study, the density of the CO_2 saturated rapeseed oil increases from 888 to 902 kg/m^3 ($\Delta\rho$ = 14 kg/m^3) between atmospheric pressure and 50 bar CO_2 at 60 °C and from 877 to 886 kg/m^3 ($\Delta\rho$ = 9 kg/m^3) at 80 °C. Based on these measurements, the density of CO_2 saturated rapeseed oil increases with CO_2 pressure and decreasing temperatures.

In [23], the density change of ten different hydrocarbons are studied at 25 °C and ambient pressure. The density change is defined as ($\rho_{degassed} - \rho_{saturated}$), where $\rho_{saturated}$ is for six different gases, including CO_2. In general, as the hydrocarbons are saturated with CO_2 the density of the hydrocarbon increases significantly.

Based on [20] and [23] the density of the Hydrofaction™ would probably increase with increasing CO_2 concentrations.

In summary, the density of the Hydrofaction™ oil needs to be decreased to reach a sufficient separation between the oil (oil/MEK) and aqueous phase, which can be achieved by diluting the oil in MEK. To demineralise the oil, which is believed to contain inorganic materials in the form of carboxylates, the pH value is lowered by CO_2(aq) to protonate the carboxylates. CO_2 could cause complications in the process in terms of changing the densities of the liquid phases. In the design of the process the oil phase floats on top of the aqueous phase, and the probable CO_2 associated density increase of the oil phase could cause the phases to shift position. Besides, CO_2 is more soluble in MEK than in water, which could cause lower concentrations of CO_2 in the aqueous phase, and reducing the demineralisation, as CO_2 reacts with water to form H^+. CO_2 as an acidification agent and MEK as a diluent are tested in the experimental work of this project.

4 Continuous Experiments

In this chapter the objective and set-up of the continuous experimental campaign for vessel 2 and 3 of the CSD is presented and the results are discussed.

The objective for the continuous campaign is to achieve knowledge about the CSD and in general the separation and demineralisation process. It is expected that the operation of the CSD in the experiments would involve manual adjustments of several components, such as opening/closing valves and calibration of the conductive level sensors. The results from the experiments would then be affected by these instabilities. The many variables are both a downside when developing the process, but it is also an eyeopener for how controllable the process is in continuous mode.

4.1 Set-up for the Continuous Experiments

Figure 4.1 illustrates the set-up for the continuous experimental campaign. The campaign focuses on the operation of vessel 2, and 3 of the CSD as this is the next step in the commissioning of the CSD, and it is also in these vessels the possible complications associated with MEK and CO_2 occur.

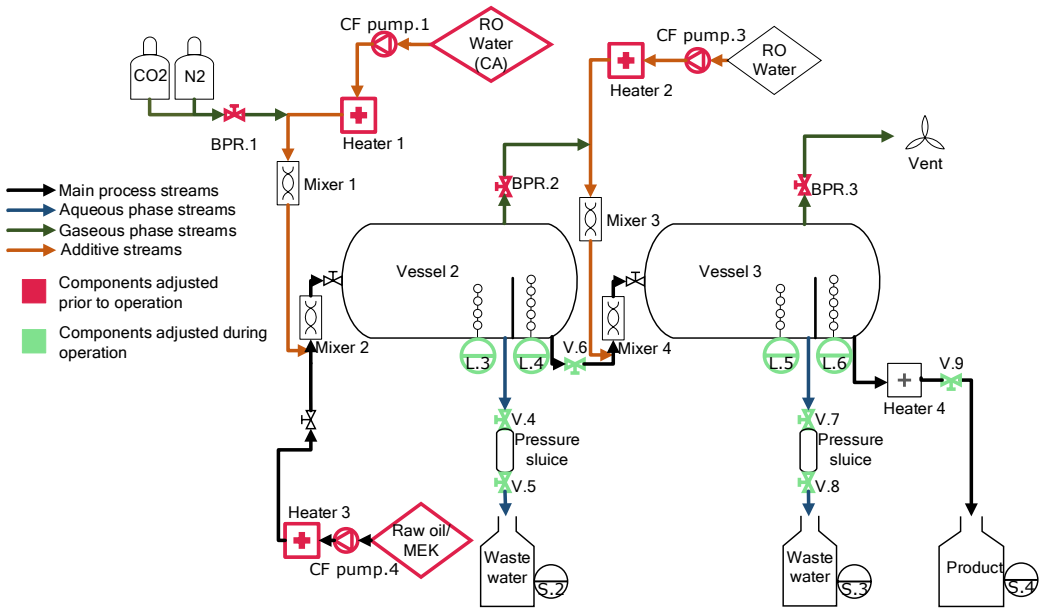

Figure 4.1: Illustration of the CSD components in operation for the continuous experiments.

The components, which are adjusted before the operation, control the temperature, pressure, flow rates and the additives.

- Temperatures are adjusted by the heaters (Heater.#) and heat tracing, which is mounted on the vessels and lines between the vessels.
- Pressures are adjusted by the Back Pressure Regulator (BPR.#).
- Flow rates are adjusted by Continuous Flow pumps (CF pump.#)
- Solutions with additives are prepared before operation.

The components, which are adjusting during operation, control the liquid extraction system. Settings for the conductive level sensors are altered to detect the interfaces between the phases, which regulates the needle and sluice valves.

4.1.1 Operating conditions

In the continuous experiments, several operating conditions are altered to reach stable operation. The method of the experimental campaign is to try different conditions, and from observations and measurements, the next experiment in the campaign is then planned. This method is justified as it is a new state-of-the-art plant.

Note that in some experiments, CA is used to acidify the environment together with CO_2 to study its effect in continuous mode and its interaction with the dissolved CO_2. In all experiments, the oil phase is diluted in MEK before the mixture is pumped into vessel 2, as the density of the oil phase needs to be lowered.

To get an overview of the adjustable operating conditions and how they are expected to affect the separation and demineralisation process, Table 4.1 is presented.

Temperature	**Increase**	• Improves separation as the density difference between the oil phase and the aqueous phase is expected to increase. • Reduces water content in the oil according to Stokes law on sedimentation speed, due the expected increase in density difference between the water and oil in the emulsion, and the lowered viscosity of the oil. • Reduces demineralisation as the solubility of CO_2 in water decreases according to Henry's law and Henry's constant for water.
CO_2 pressure	**Increase**	• Improves demineralisation as the solubility of CO_2 in water increases with increasing pressures according to Henry's law. • Reduces water content in the oil due to the destabilisation of the oil emulsion. • Reduces separation due to a possible decrease in density difference between the oil and aqueous phase as more CO_2 is possibly dissolved in MEK than in water.
Oil/MEK (feed) flow rate	**Increase**	• Reduces demineralisation due to decreasing retention times. • Increases water content in oil due to decreasing retention times.
RO water flow rate	**Increase**	• Could reduce the separation and demineralisation and increase water content in the oil by decreasing the retention time of the oil phase. This would depend on the stability of the process. As more water enters the vessels, more need to be extracted from the vessels, and if the extraction rate is too fast, the pressure inside the vessels drop and reduces demineralisation.
Concentration of MEK in feed	**Increase**	• Uncertain impact: MEK dilutes the oil, which increases the density difference between the aqueous phase and the oil phase, and improves separation. However, CO_2 is more soluble in MEK than in water according to their Henry's constants, which could increase the oil phase density and by that lower the density difference between the aqueous and oil phase. • Reduces demineralisation due to the increase of CO_2 concentrations in MEK. Less CO_2 dissolved in is the aqueous phase and the acidification of the environment is reduced.
Addition of CA	**Yes**	• Improves separation and demineralisation due to the increased acidification of the environment.

Table 4.1: Expected impact on separation and demineralisation performance with changing operating conditions.

4.2 Results

During the campaign, different feeds have been used, and they differ in inorganic, water and MEK content, which are measured and presented in Table 4.2.

The inorganic content of the oil emulsion is associated with its measured ash content. A measure of the ash content is achieved by combusting all compounds of the sample up to 775 °C. The remaining product is then called the ash content of the sample. In the tables below the ash content are presented, and it is assumed that these values are equal to the inorganic content.

	Ash [wt.%]	Water [wt.%]	MEK [wt.%]	Ash (MEK free) [wt.%]
Feed 1	0.48	9.7	52.8	1.02
Feed 2	0.08	6.3	61.8	0.21
Feed 3	1.15	4.4	60.0	2.88
Feed 4	1.52	5.8	67.9	4.75

Table 4.2: The different feed for the continuous experimental campaign.

The Ash (MEK free) values are the estimated ash content in the oil and water of the product. It is calculated by the equation below. Based on the analysis in Section 3.1, it is justified that the inorganic content of the product sample is situated in the oil and water part of the product samples.

$$Ash(MEKfree) = \frac{Ash_{measured}}{1 - MEK_{measured}}$$
$$Ash(MEKfree)_{feed1} = \frac{0.48wt.\%}{1 - 52.8wt.\%} = 1.02wt.\%$$

As presented in Table 4.3 eight continuous experiments are performed in the campaign, and 14 product samples are taken. Additionally, samples are of the waste water from vessel 2 and 3, ww2 and ww3, are taken.

			Operating conditions								Analysis results				
Exp #	**Sample #**	**Feed #**	**Feed flow [kg/h]**	**RO-2 flow [kg/h]**	**RO-3 flow [kg/h]**	**Temp-2 avg [°C]**	**Temp-3 avg [°C]**	**Pressure-2 avg [bar]**	**Pressure-3 avg [bar]**	**CA solution 0.1 M**	**Ash [wt.%]**	**Water [wt.%]**	**MEK [wt.%]**	**Ash (MEK free) [wt.%]**	**Water (MEK free) [wt.%]**
1	**1**	1	4.3	4.0	4.0	52.7	51.4	29.4	24.3	No	0.66	4.7	30.6	0.96	6.8
	2	1	4.3	4.0	4.0	52.6	51.5	27.2	23.8	No	0.05	4.7	30.6	0.07	6.8
2	**3**	1 and 2	4.3	4.0	4.0	52.6	51.8	27.5	23.6	No	0.16	5.3	30.6	0.23	7.6
	4	2	4.3	4.0	4.0	52.1	52.1	27.6	23.3	No	0.05	4.4	30.6	0.07	6.3
3	**5**	2	3.0	2.5	5.0	50.6	49.6	29.2	24.0	No	0.04	4.4	42.5	0.07	7.7
	6	2	2.8	2.5	5.0	50.5	49.7	29.1	24.2	No	0.08	4.7	42.5	0.14	8.2
4	**7**	2	3.0	2.5	5.0	51.2	49.2	34.6	28.1	No	0.03	5.0	50.7	0.06	10.2
5	**8**	2	2.5	2.5	2.5	50.2	50.1	34.6	29.8	No	0.06	4.9	47.9	0.12	9.3
	9	2	2.5	2.5	2.5	50.2	50.1	34.6	29.8	No	0.11	5.9	47.9	0.21	11.3
6	**10**	3	3.0	2.3	2.3	18.3	24.0	15.8	18.7	Yes	0.59	4.5	52.2	1.23	9.5
	11	4	2.9	2.4	2.3	18.3	22.0	18.4	13.4	Yes	0.19	4.7	64.4	0.53	13.1
7	**12**	4	2.9	2.4	2.3	18.3	21.7	18.4	13.1	Yes	0.05	4.9	64.4	0.14	13.9
	13	4	2.9	2.4	2.3	18.3	21.7	18.4	13.1	Yes	0.12	4.9	64.4	0.34	13.7
8	**14**	4	2.9	2.4	3.0	17.4	17.9	18.9	13.4	Yes	0.01	6.9	66.0	0.03	19.1

Table 4.3: Data from the continuous experimental campaign. Ash and water content of the oil phase is displayed together with the operating conditions for each sample. The gray boxes are described below in the data quality section.

From Table 4.3, the water content in the product sample is nearly constant at 5 wt.% for all samples. The reason for lower values are not achieved, could be explained by the solubility of water in MEK. At 25 °C the solubility of water in MEK is 0.12 gWater/gMEK [24]. It is not believed that the pressure would affect the solubility considerably, due the fact that the liquids are rather incompressible and the pressure does not affect the MEK in water solubility considerably, as illustrated in Figure 3.3. The water content of the product sample can be estimated by the equation below if it is assumed that all water is situated in the MEK part of the product.

$$\begin{aligned} Water_{content} =& WaterInMEK_{solubility} \cdot MEK_{concentration} \\ =& 12[wt.\%] \cdot 30[wt.\%] \ to \ 66[wt.\%] \\ =& 3.6[wt.\%] \ to \ 7.9[wt.\%] \end{aligned}$$

The estimated concentrations of water in the MEK of the product samples fit well into the constant measured 5 wt.%.

In Table 4.3, the presented values in the Water (MEK free) - column, can be assessed as if the water content of the product samples are situated in the oil part of the sample. Due to the variation in MEK concentrations of the product samples, these values vary as well; from 6.8 wt.% to 19.1 wt.%.

It is difficult to assess how the equilibrium of water in the oil phase behaves when both MEK, oil compounds, CO_2(aq), inorganics, and in some experiments, CA, are a part of the phase. Due to this difficulty, the water content in the oil is inaccurate, and further water analyses and measurements on MEK free product samples need to be conducted.

In Table 4.3, the MEK free ash values of 0.06 and 0.07 wt.% for product sample 2, 4, 5, 7 are displayed. Ash content below 0.1 wt.% have never been achieved before for a Hydrofaction™ oil in batch-wise lab-scale experiments with CO_2 as acidification agent. These ash content values are promising for the continuous separation and demineralisation process. Due to unstable operations the ash content of the product samples are not consistent. In experiment number 2, an ash content of 0.07 and 0.23 wt.% is obtained, which can be caused by unstable operations.

To compare product samples from different feeds, the relative reduction/increase in ash content is calculated. The calculations are based on the MEK free ash content due to the considerable variation in MEK concentrations, and the assumption that the inorganic content are situated in the oil and water part of the samples.

$$Reduction(MEKfree)_{ash} = \frac{Feed(MEKfree)_{ash} - Sample(MEKfree)_{ash}}{Feed(MEKfree)_{ash}}$$

Exp #	Sample #	Feed #	Ash reduction [%]
1	**1**	1	7
	2	1	93
2	**3**	1 and 2	65
	4	2	66
3	**5**	2	67
	6	2	34
4	**7**	2	70
5	**8**	2	45
	9	2	-1
6	**10**	3	57
	11	4	89
7	**12**	4	97
	13	4	93
8	**14**	4	99

Table 4.4: Calculated relative reduction for ash content in the product samples (MEK free) when compared to its feed.

From Table 4.4, the overall impression of the demineralisation is positive. 10 out of 14 ash reduction results are above 50 %, and one is 99 %. The stability of the process needs to be improved as the ash reduction values vary from -1 % to 99 %. The value of -1 % could be caused by uncertainties in the measurement of the ash content or the procedure for how the sample is collected.

pH measurement of ww2 and ww3 are presented in Table 4.5. The lowest pH measurements are observed in the experiments with CA. It is possible that lower pH values for the experiments with only CO_2 are achieved in the vessels as the ww2 and ww3 samples are taken at ambient pressure and the vessels are pressurised. The pH value, related to CO_2 acidification is highly dependent on pressure and a potentially pH value of 3 could have been reached inside the vessels.

Exp #	pH ww2	pH ww3	0.1 M CA solution
3	7.6	6.5	No
4	7.1	6.4	No
6	3.3	3.1	Yes
7	4.5	5.7	Yes

Table 4.5: pH measurements of ww2 and ww3. The experimental numbers are associated with experiment numbers of product samples in Table 4.3 and 4.4.

The pH value for ww3 is lower than the one for ww2 in experiment 3, 4 and 6. As either CO_2 or a CA solution acidifies the environment in the vessels, the carboxylates are protonated and release its alkali metal. A higher concentration of inorganics in the oil would increase the protonation and reduce the concentration of H^+ in the environment, which possibly can be observed by increased pH values. This explanation could be the reason why the pH value is higher for ww2 than for ww3, as a higher inorganic content is expected to enter vessel 2. For experiment 7 it is opposite; ww3 has a higher pH value than ww2. This could indicate a better demineralisation in vessel 3 than in the vessel 2. Unstable operations, such as poor acidification, could be the cause for the high pH value for ww3.

4.2.1 Data Quality

It is essential to study the quality of the data to interpret the significance of the data before analysing the expected impacts, presented in Table 4.1, by evaluating the results from this campaign.

- **MEK concentration:** Some of the MEK concentrations are in gray in Table 4.2. These values are estimated based on measurements on similar product samples from the same experiment. The MEK concentration measurements are attained by evaporation of the product samples. The evaporation set-up is further described in Appendix B.
- **Flow rates:** The flow rates in grey in Table 4.3 are estimated from a pump curve produced by Steeper Energy. The pump curve is based on an experimental study on the CF pumps used in the CSD. The non-grey values are measured during the experiments.
- **Temperature and pressure:** The values for temperature and pressure are averaged based on the duration of each sample.

Stable and Unstable Operation

Both stable and unstable operation is observed during the campaign. An example of a rather stable operation, though still with separation issues, is visualised in Figure 4.2 and an example of a more unstable operation is visualised in Figure 4.3

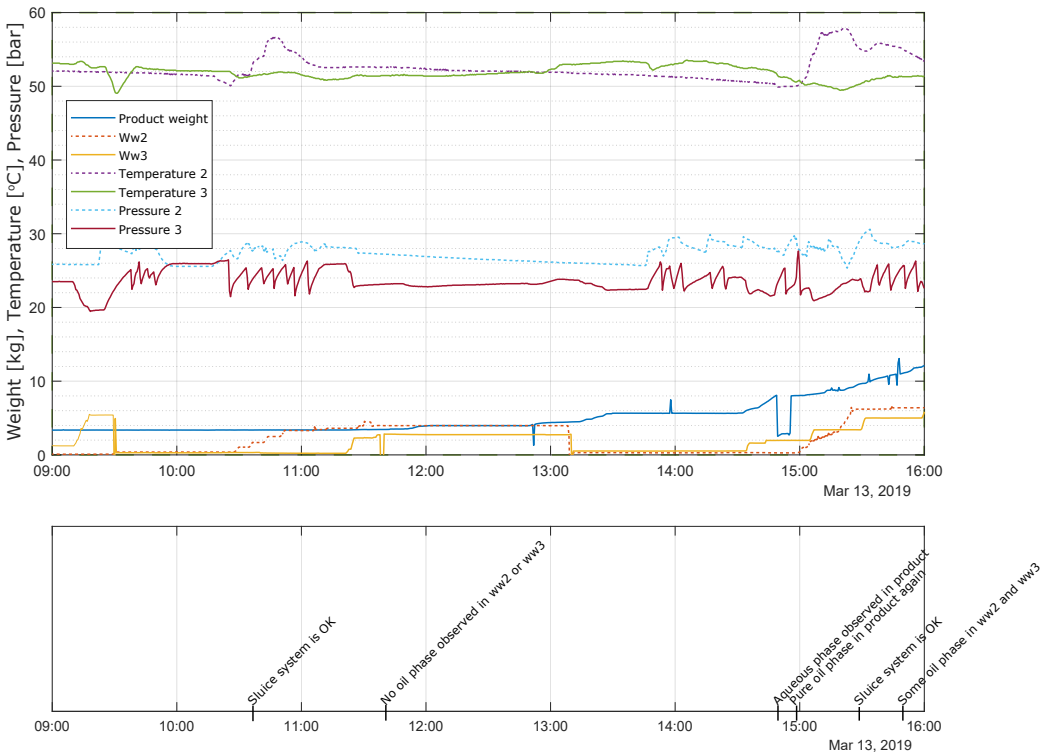

Figure 4.2: Raw data from experiment number 2. The numbers, 2 and 3 in the legend, refer to vessel 2 and 3, respectively. Temperature and pressure are measured inside each vessel. Ww and product weight are measured by online scales.

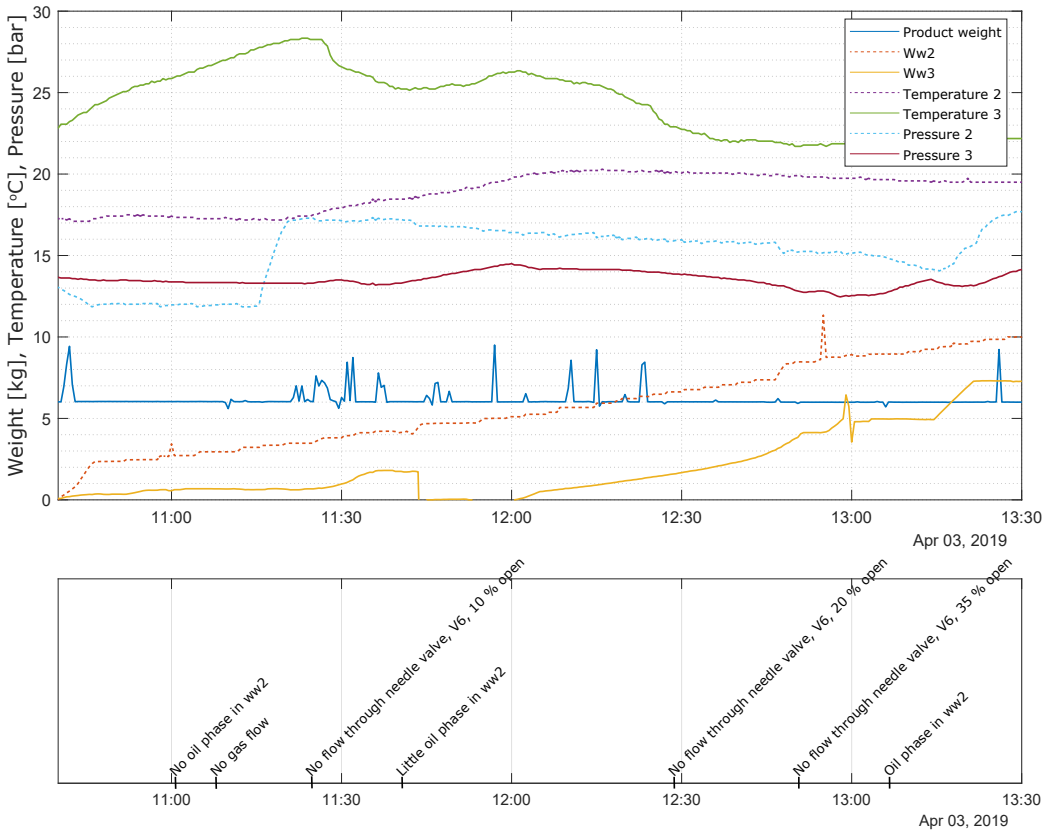

Figure 4.3: Raw data from experiment number 6.

From Figure 4.2 and 4.3, multiple operational complications can be observed.

- **Gas flow:** Due to a large consumption of CO_2 in the experiments and little CO_2 in stock, the CO_2 flow was unstable. A constant CO_2 flow is preferred, as it is expected that mixing the CO_2 with RO water prior to entering the vessels would increase the concentration of CO_2 in the water and improve demineralisation.

- **Manual operation of valves:** The conductive level sensors control the valves for extracting the liquids. The sensors became dirty, and it was hard to detect the interfaces. In some experiments, the extraction of the aqueous phase was performed manually by the operator, and the rate of extraction was based on inflow rates.

- **The needle valve, V.6:** The operation of the needle valve, which controls the oil phase flow between vessel 2 and 3, was performed manually in all experiments. It is not possible to monitor the flow rate between the two vessels, however by observations on the conductive level sensor, L.4, it can be assessed if the valve is opened or closed. In some cases, the needle valve was blocked, which resulted in opening the valve more (visualised in Figure 4.3). This caused the oil phase flow from vessel 2 to vessel 3 to be unsteady.

Due to unstable operation in some of the experiments and thereby a decrease in data quality, the results from the continuous campaign are interpreted as guidelines for further commissioning of the CSD and understanding of the Hydrofaction™ separation and demineralisation process. The tendencies below can be inaccurate as the operational parameters are not isolated, and the ash reduction of the oil are a function of multiple operational parameters. The water content in the oil measurements are considered too inaccurate and is not a part of the tendency analysis.

4.3 Tendencies

The expected separation and demineralisation impacts from Table 4.1 are studied in this section. The ash reduction values from Table 4.4 are compared with operating conditions from Table 4.3.

4.3.1 Ash Reduction vs CA and Temperatures

From Table 4.3 it can be observed that for product sample number 1 to 9, no CA solution is used in the experiments and for product sample number 10 to 14 a 0.1 M CA solution is used. The 0.1 M CA solution is prepared before the operation and is pumped into vessel 2 during operation. As the CA solution acidifies the environment, the separation and demineralisation are expected to be improved.

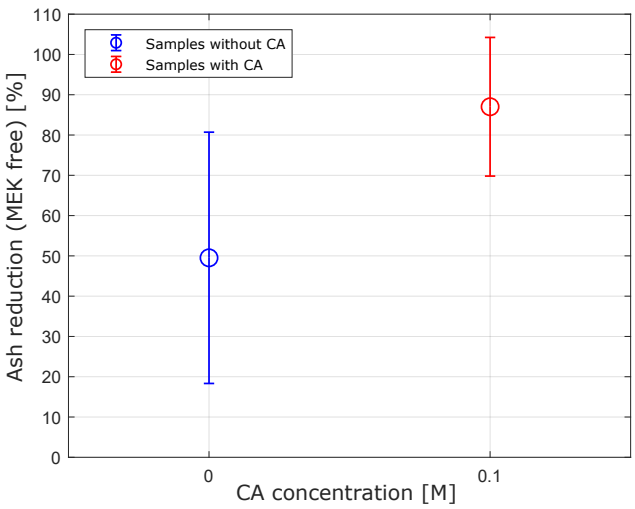

Figure 4.4: Error bar plot for relative ash reduction vs concentration of CA. The concentration of CA is either 0 or 0.1 M - no concentrations in between are used in the campaign.

From Figure 4.4, the reduction of ash increases with CA concentrations, which is as expected due to the higher demineralisation rate when the acidification of the environment increases. However, the same tendency is observed with decreasing temperatures, as illustrated in Figure 4.5. Unfortunately the experiments at low temperatures are the ones with CA and the experiments with high temperature are the ones without CA. No experiments with temperatures in between low (18 °C) and high (55 °C) temperatures exist. It is not possible by examining the campaign data to determine how CA and temperature affect ash reduction.

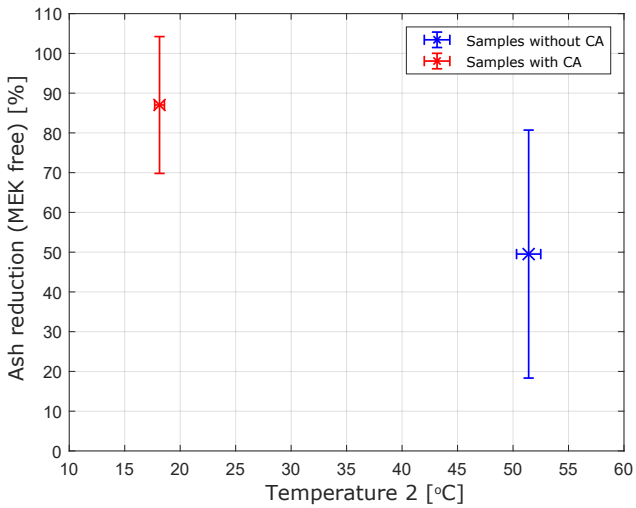

Figure 4.5: Error bar plot for relative ash reduction vs average temperature in vessel 2.

4.3.2 Ash Reduction vs Pressures, Flow Rates, and MEK Concentrations

From Figure 4.6 it is inconclusive how the pressure in vessel 2 affects the ash reduction and thereby the demineralisation. The same inconclusiveness is valid for the ash reduction with flow rates and MEK concentrations.

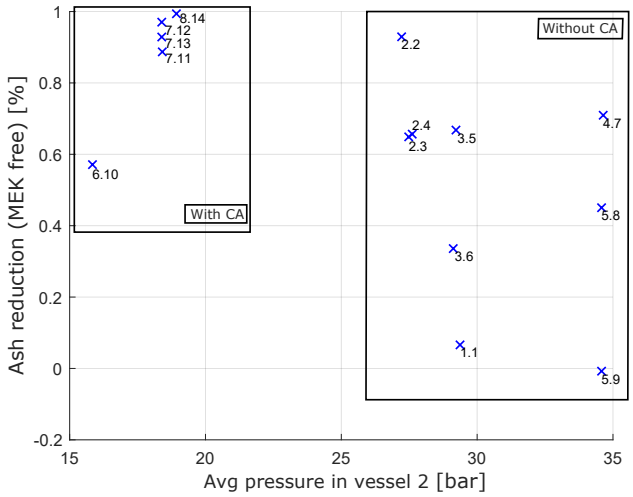

Figure 4.6: Ash reduction vs average pressure in vessel 2. The data points are labeled; The first number refers to the experiment, and the last number refers to the product sample number.

Promising results have been achieved in the continuous experimental campaign in terms of ash reductions of the Hydrofaction™ oil. However, due to unstable operations, it is not possible to assess how operating conditions affect the separation and demineralisation process of the CSD. One of the main unstable behaviours of the CSD is phase shifting. The oil phase is observed in ww2 and ww3 and aqueous phase is observed in the product. A better understanding of the phases and why they can shift position is needed, which is why the batch experiments are conducted and are presented in the next chapter.

5 Batch Experiments

In this chapter the objective and set-up for the batch experimental campaign are presented and its results are discussed.

In the continuous experiments, unstable operation is observed, and to get a better understanding of the CSD, batch experiments are conducted. The knowledge from the batch experiments should eventually lead to a more stable operation of the CSD in the future.

5.1 Motivation

The motivation for this study is unstable operations in the continuous campaign, where phase shifting is observed, i.e. the oil phase becomes the bottom phase and the aqueous phase becomes the middle phase. Figure 5.1 illustrates a continuous experiment where phase shift has occurred.

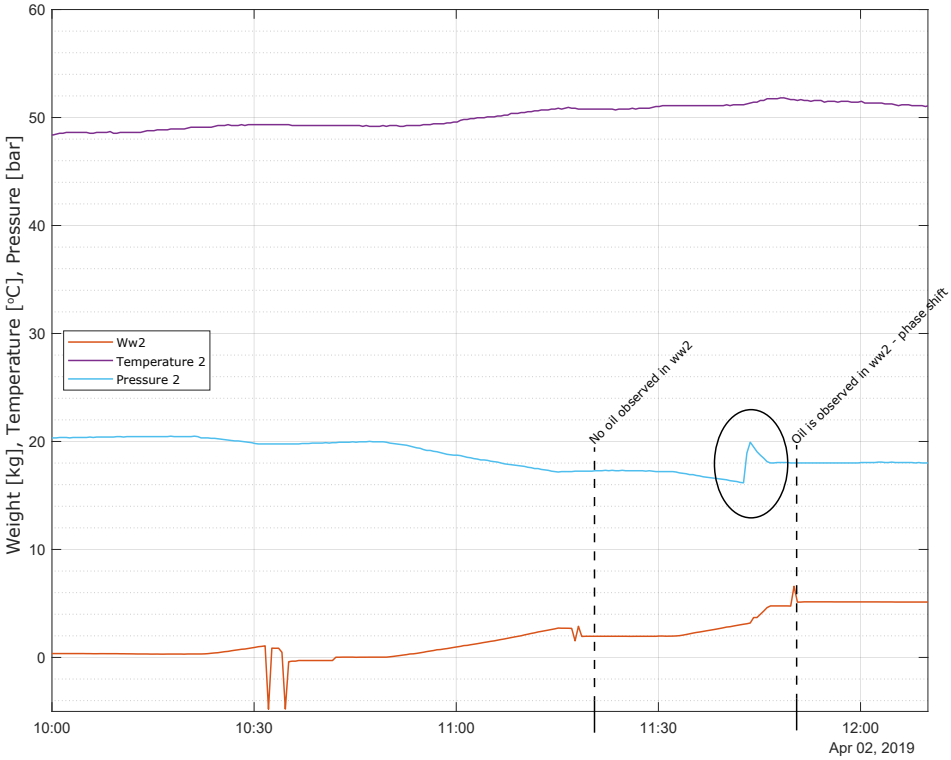

Figure 5.1: Raw data from a continuous experiment. Two moments in the experiment are marked - one where only the aqueous phase is observed in ww2 and one where both the aqueous and oil phase is observed in ww2. The black ellipse between the two observations marks a sudden pressure increase in vessel 2.

Based on the observation in Figure 5.1 and the analysis in Section 3.4 and 3.5, it is postulated that a sudden increase in CO_2 pressure can cause the liquid phases to shift position. As the oil phase is floating on top of the aqueous phase, the oil phase is directly exposed to the CO_2 pressure increase. If density increases with CO_2 concentrations in the oil phase, it becomes denser, and possibly more dense than the aqueous phase, causing the phases to shift position. The solubility of CO_2 is studied by blank experiments to determine the solubility of CO_2 in RO water and feed (oil/MEK solution).

5.1.1 Set-up

The experiments are conducted in vessel 2 as it is possible to pump three different additives directly into the vessel. Two blank experiments are conducted; one with RO water and one with an oil phase with 60 wt.% MEK, which is similar to the feeds used in the continuous campaign. Figure 5.2 illustrated the components, which is used for blank experiments.

The procedure for performing the two blank experiments is identical.

- The feed or RO water is pumped into vessel 2. To compare results from the two blank experiments, the liquid amounts pumped into vessel 2 are similar. The amount of liquids are visualised in Figure 5.2 and is approximately 10 L.
- The vessel is pressurised with 40 bar CO_2.
- The pressure and temperature, when steady, are noted.
- To study the effect of temperature, the temperature is set to increase, which is achieved by the heat tracing, mounted on the vessel. The two blank experiments are divided into two sub-experiments; one cold (20 °C) and one hot (55 °C). The vessel is not emptied between the two sub-experiments.
- The pressure and temperature, when steady, are noted.

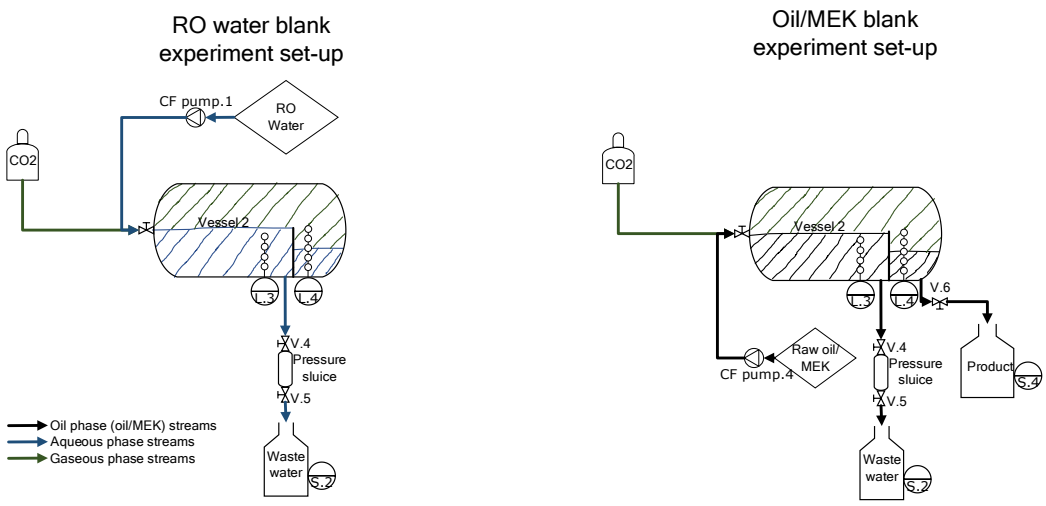

Figure 5.2: Illustration of the blank experiments on vessel 2.

The expected impacts on the CO_2 solubility in the liquids in relation to operating conditions are presented in Table 5.1. In addition to these expected impacts, it is also expected that more CO_2 is dissolved in the feed than in the RO water, due to the large amount MEK in the feed.

Temperature	**Increase**	• Decreases solubility of CO_2 in the liquid phases. according to Herny's law.
CO_2 pressure	**Increase**	• Increases solubility of CO_2 in the liquid phases. according to Henry's law.
Duration	**Increase**	• Increases the amount of CO_2 in the liquid phases until equilibrium is reached.

Table 5.1: Expected impact on CO_2 solubility with changing operating conditions.

5.2 Results

Raw data of the temperature and pressure in vessel 2 from the blank experiments are presented in Figure 5.3 and 5.4 as a function of hours.

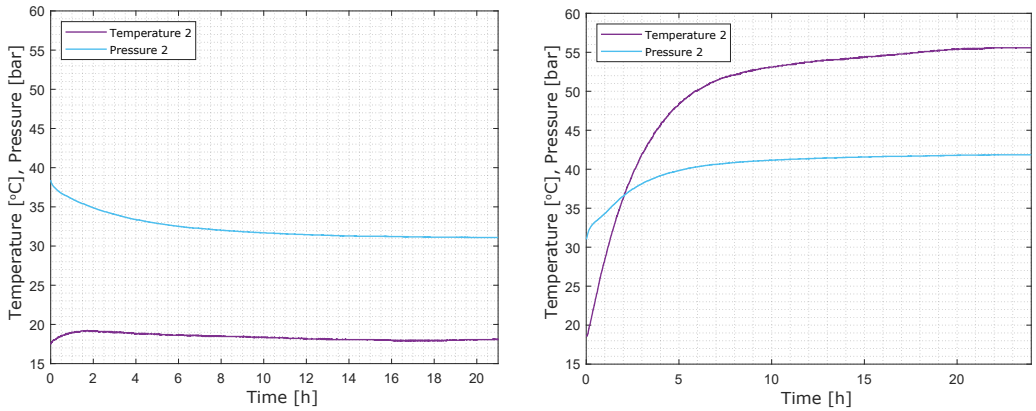

(a) RO water blank cold. **(b)** RO water blank hot.

Figure 5.3: Raw data from the blank experiment with RO water.

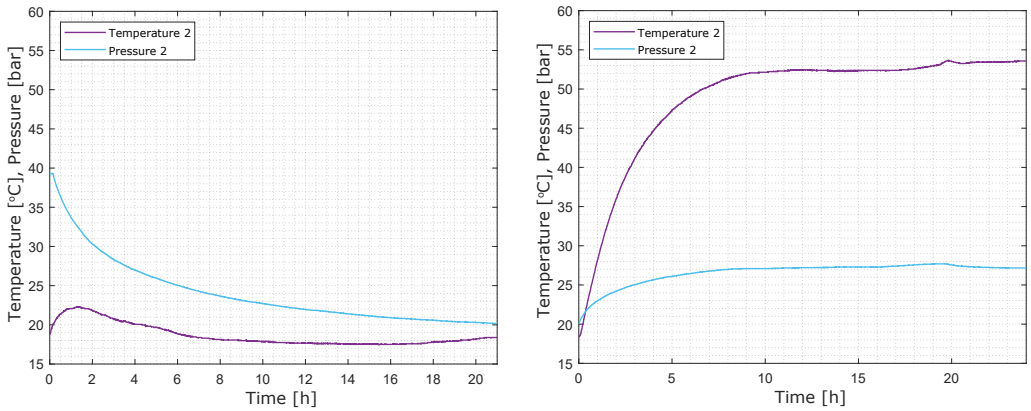

(a) Feed blank cold. **(b)** Feed blank hot.

Figure 5.4: Raw data from the blank experiment with the feed.

From the cold experiments in Figure 5.3a and 5.4a, the CO_2 pressure decreases faster and more for the feed experiment than for the RO water experiment. This indicates a higher solubility of CO_2 for the feed, and a higher rate of dissolution, which is expected. For the cold feed experiment, a steady pressure is not reached within the duration of the experiment (21 hours), and it is possible that a higher concentration of CO_2 could have been reached. The pressure for the cold RO water experiment is almost steady after 12 hours.

In the hot blank experiments, illustrated in Figure 5.3b and 5.4b, the pressure increases when the temperature increases, as they are a function of each other. However, it is not clear if CO_2 escapes the liquids and add on to the pressure increase. According to Henry's law in Equation 3.11 and Henry's constants for pure water and MEK in Table 3.2, it is expected that CO_2 escapes the liquids as temperature increases.

5.2.1 Henry's Constants

To further study the solubility of CO_2 in the liquids, Henry's constants are calculated for each experiment. The noted temperatures and pressures for the blank experiments are presented in Table 5.2, together with the calculated mole fraction of CO_2 in the liquid phases.

Exp	Pressure start [bar]	Pressure end (steady) [bar]	Temp start [°C]	Temp end (steady) [°C]	Liquid volume [L]	Gas volume [L]	Mole fraction [%]
Blank-feed-cold	39.3	20.1	18.8	18.5	9.6	16.4	4.1
Blank-feed-hot	20.1	27.2	18.5	52.5	9.6	16.4	3.5
Blank-ROwater-cold	38.4	31.0	17.6	18.6	9.5	16.5	1.7
Blank-ROwater-hot	31.0	41.2	18.6	53.3	9.6	16.4	1.0

Table 5.2: Data from the blank experiments. The liquid volume of the oil phase is calculated based on the assumption that the density of the feed is 900 kg/m^3 (based on the 60 wt.% MEK concentration in the feed). The mass of the feed in the vessel is known and is 8.6 kg The volume of the RO water is based on the calculated density of water from the thermophysical property functions in EES® and the known mass of RO water in the vessel, which is 9.5 kg. The remaining volume inside the vessel is then occupied by the CO_2(g). The mole fractions are calculated based on CO_2 densities also from the thermophysical property functions in EES®.

From the mole fractions in Table 5.2, Henry's constant can be calculated by Equation 3.11. In Table 5.3 the Henry's constants from the blank experiment are presented together with the constants for CO_2 in pure water and CO_2 in MEK.

Exp	Exp Henry's constant [bar]	Henry's constant based on [16] (CO_2 in pure water)	Henry's constant based on [26] (CO_2 in MEK)
Blank-feed-cold	487	1434	54
Blank-feed-hot	772	2971	90
Blank-ROwater-cold	1833	1441	54
Blank-ROwater-hot	4307	3007	91

Table 5.3: Henry's constants for the blank experiments. The literature based Henry's constants are calculated based on the steady temperature in each experiment. The calculations are further described in Appendix C

In Table 5.3, the Henry's constants for CO_2 in RO water experiments are higher than the ones found in the literature for pure water, which could be explained by the expected increased Henry's constants for brines, as presented in Table 3.2. It is an uncertainty for the RO water experiments. However, it is possible that due to remains of inorganics in the vessel and pipes, some of the inorganics are dissolved in the RO water.

In appendix D, the solubility of CO_2 in the oil phase of the feed is assessed. Based on Henry's constants, steady temperatures and pressures in Table 5.3, the known mass of MEK in the vessel (5.2 kg), and density calculations on the phases from the thermophysical property functions in EES®, the estimated masses of CO_2 in the MEK part of the feed are 1.2 and 1.0 kgCO_2 in the cold and hot experiment, respectively.

The calculated masses dissolved in the feeds are 0.9 and 0.8 kgCO_2 (calculations also presented Appendix D) for the cold and hot experiment, respectively. Based on the calculations, all the dissolved CO_2 can be dissolved in the MEK part of the feed, and the MEK would not be saturated. No CO_2 is dissolved in the oil phase of the feed. However, as the oil phase and MEK mix, the mixture solubility could change. There is also some water in the oil phase, which could lower the mixture solubility.

In summary, the CO_2 solubility in RO water is between 2.4 and 3.5 times lower than the CO_2 solubility in the feed, based on the mole fraction calculations in Table 5.2. Literature on how the density of MEK changes with CO_2 concentrations have not been found, however, the density of pure water, NaCl aqueous solutions, rapeseed oil and some hydrocarbons have been observed to increase with CO_2 concentrations, and it is likely that MEK increases with CO_2 concentrations as well. This indicates that the initial intention with diluting the oil in MEK to decrease its density could be counteracted by the addition of CO_2 in the process. Additionally, the Hydrofaction™ oil possibly has a lower CO_2 solubility than MEK, and another diluent should perhaps be used in the separation and demineralisation process in the presence of CO_2 as the acidification agent.

6 Further Development

In this chapter, the further development of the separation and demineralisation process is discussed. The discussion is based on the issues observed during the CSD experiments, potential solutions are proposed.

The set-up for the continuous experimental campaign is presented in Figure 6.1 to visualise, where the operating issues have been observed and what key components are problematic.

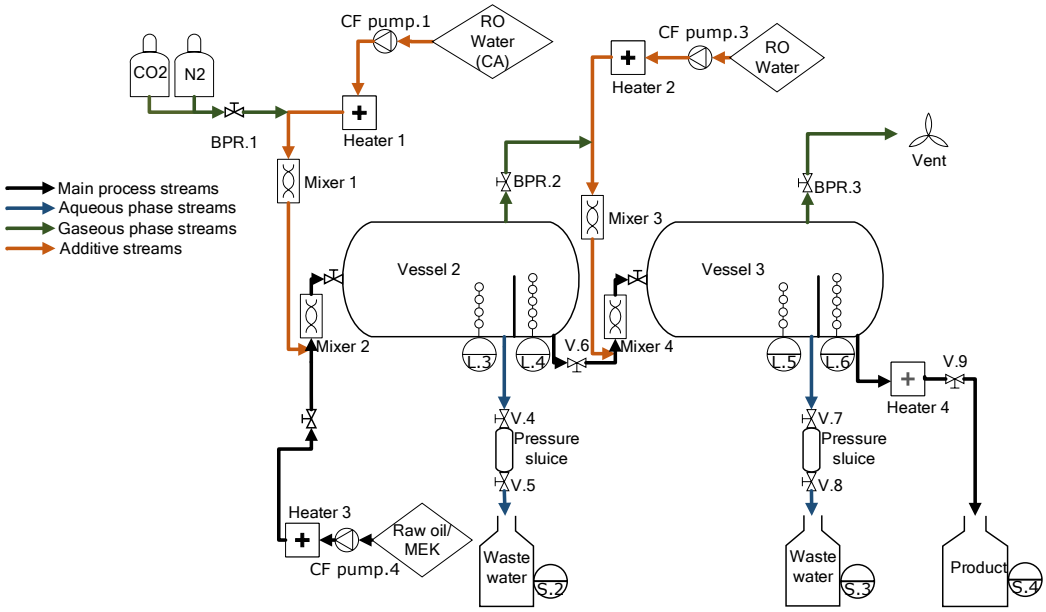

Figure 6.1: The set-up for the continuous experimental campaign.

The unstable operations observed during this project can be associated with different components and/or additives of the CSD.

- **Conductive level sensors (L.3 to L.6 in Figure 6.1):** It has been observed that the conductivity of the liquids in the vessels vary with both temperature, pressure, and presence of CO2, diluent, amount of oil in water and amount of inorganics in both water and oil. The variations in electric conductivity of the different phases make level detection and control of the different phases difficult. In some cases, there is only a small difference between the conductivity of the oil and aqueous phase, and thus the operator needs to adjust the sluice control carefully in order to detect the water/oil interphase correctly. It is believed that the small difference could be caused by the design of the level sensor, as the oil phase tend to stick to the electrodes measuring the conductivity, and the sensors need to be cleaned. A new design for the interface detecting sensors is needed, and it does not necessarily need to detect the conductivity of the phases. Often level sensors are based on density differences, but as the densities have also been observed to vary significantly, this is not an optimal parameter to base the measurement on. The guided wave radar, which uses the difference in dielectric constants of the phases to detect the phase interface, is an appealing technique. It sends pulses of microwaves through the phases, and the received reflected pulses are dependent on the dielectric constants of the phases. A significant advantage of this technique is that it can be mounted from the top of the vessel, and there is little cleaning maintenance.

- **Phase shift:** The observed phase shift in separator vessels are crucial to address, as the liquids need to be extracted through its outlets. It is proposed in this project that changing densities of the oil and aqueous phase are involved in the phase shift behaviour. Oil is diluted in MEK to lower its density, which is necessary as the oil phase should float on top of the aqueous phase. The solubility of the acidification agent, CO_2, in MEK is significantly higher than its solubility i pure water. This CO_2 in MEK attraction could cause undesirable density changes of the oil phase, as it is believed that its density increases with CO_2 concentrations, which could cause the phase shift. As more of the dissolved CO_2 end up in the oil phase, less are dissolved in the aqueous phase, which could reduce the demineralisation performance, as less CO_2 would react with water to form the pH-reducing H^+. It is possible that a new diluent is needed to dilute the oil when CO_2 is presence as the acidification agent.

  Another plausible cause of the phase shift behavior could be the design of the sluice system, which is illustrated in Figure 6.1 by two valves with a pressure sluice in between. When the first valve opens, it sucks aqueous phase into the sluice. It is not known from which direction the aqueous phase is sucked

from. If the direction is straight up it could be imagined that the top floating oil phase can be sucked into the sluice as well, which would be observed as an phase shift by the operator. To avoid this a plate can be mounted with a given length from the outlet to guide the aqueous phase into the outlet from the sides.

- **Flow rates between vessels:** The flow rate of the oil phase between vessel 2 and 3 is difficult to control, which induces issues in terms of controlling the mixing ratio between RO water and the oil phase for vessel 3. Blocking of the needle valve has been observed, which in most cases is fixed by moving the needle of the valve. However, the operator does not have a flow measurement, and it is not obvious when the valve is blocked. Thus a potential solution could be a flow-meter mounted in connection with the needle valve. The blocking issue would though, possibly still be present. Another solution could be controlling the flow with a pump. The pump should be able to withstand the temperatures, pressures and possibly a diluent.

7 Conclusion

The focus in this project is to gain knowledge on the continuous phase separation of liquefaction products and demineralisation of liquefaction oil in the presence of CO_2 as an acidification agent. This work is the next step in the development of the process and has been conducted experimentally on the pilot-scale continuous separation and demineralisation system. This system is based on Steeper Energy's proprietary Hydrofaction™technology. Previously, the process has been developed in lab-scale batch reactors, where operating conditions are somewhat controllable. Going from lab-scale batch reactors to continuous pilot-scale experiments increases the complexity significantly.

The increased complexity of the continuous system affects the operational stability of the experiments. Due to, among others, phases shift position in the separator vessels and inconsistent flow rates, unstable operations were observed. It is thereby difficult to conclusively determine how operating conditions are affecting the separation and demineralisation process from the experiments presented in this report. It is necessary to understand why these instabilities occur in order to stabilise the system and produce consistent results, which is why the batch experiments are conducted on the pilot-scale system. These experiments are designed to achieve knowledge on how the dissolved CO_2 could affect the stability by studying the solubility of CO_2 in the oil and aqueous phase.

From the batch experiments, the solubility of CO_2 in the oil phase are 2.4 and 3.5 times higher than the ones for CO_2 in RO water. The considerably higher solubilities are believed to be caused by the addition of density decreasing diluent, methyl ethyl ketone, in the oil phase, which can dissolve a large amount of CO_2. These observations suggest that the CO_2 tends to be dissolved in the oil phase rather than the aqueous phase, which could affect the separation process negatively, as densities presumably increase with CO_2 concentrations.

Despite the instabilities of the continuous experiments, promising results are achieved. An ash content of 0.06 wt.% of a Hydrofaction™ oil with CO_2 as the acidification agent. This reflects a 70 % reduction of inorganics during the demineralisation. Lower ash content levels have never been achieved in lab-scale batch experiments with CO_2 as acidification agent. The highest ash reduction achieved in the experiments is 99 %. This is though with both citric acid and CO_2 as acidification agents; however, the result indicates that the citric can be used in continuous mode to improve the demineralisation of the oil.

The work in this project has provided an essential knowledge-based foundation for the further development of the continuous phase separation of liquefaction products and the demineralisation of liquefaction oils with CO_2 as acidification agent.

Bibliography

[1] "Directive (EU) 2018/2001 of the European Parliament and of the Council of 11 December 2018 on the promotion of the use of energy from renewable sources (Text with EEA relevance.)," *Official Journal of the European Union,* L 328, pp 82-209, 2018.
https://eur-lex.europa.eu/legal-content/EN/TXT/?uri=uriserv:OJ.L_.2018.328.01.0082.01.ENG&toc=OJ:L:2018:328:TOC. Accessed: 07.05.2019.

[2] J. A. Lamb A. F. Hunt. "Liquid—liquid phase equilibrium in the 2-butanone—water system at high pressure," *Fluid Phase Equilibria*, vol. 3, pp. 117-184, 1979.

[3] A. A. Teixeira B. Meyssami M. O. Balaban. "Prediction of pH in Model Systems Pressurized with Carbon Dioxide," *Biotechnology Progress*, vol. 8, pp. 149-154, 1992.

[4] G. C. Maitland J. P. Martin Trusler D. Vega-Maza C. Peng J. P. Crawshaw. "The pH of CO_2-Saturated Water at Temperatures between 308 K and 423 K at Pressures up to 15 MPa," *The Journal of Supercritical Fluids*, vol. 82, pp. 129-137, 2013.

[5] *Carbon Dioxide and Carbonic Acid-Base Equilibria*.
http://ion.chem.usu.edu/~sbialkow/Classes/3650/Carbonate/Carbonic%20Acid.html. Accessed: 14.05.2019.

[6] European Commission. "Transport Emissions"
https://ec.europa.eu/clima/policies/transport_en. Accessed: 14.04.2019.

[7] European Commission. "Electrification of the Transport System - Studies and Reports." Directorate-General for Research and Innovation Smart, Green and Integrated Transport, Brussels, 2017.

[8] Randall T. Cygan. "Sandia Report: The solubility of Gases in NaCl Brine and a Critical Evaluation of Available," http://randallcygan.com/wp-content/uploads/2017/06/Cygan1991SR.pdf. SAND90-2848, UC-721, 1991.

[9] S. Bauer D. Li B. J. Graupner. "A method for calculating the liquid density for the CO2-H2O-NaCl system under CO2 storage condition," *Energy Procedia*, vol. 4, pp. 3817-3824, 2011.

[10] F. E. Massoth E. Furimsky. "Deactivation of Hydroproessing Cataysts," *Catalysis Today*, vol. 52, pp. 381-495, 1999.

[11] International Energy Agency (IEA). "Biofuels for transport" `https://www.iea.org/tcep/transport/biofuels/`. Accessed: 08.05.2019.

[12] C. U. Jensen. "PIUS - Hydrofaction™ Technology Platform with Integrated Upgrading Step, PhD Thesis." Aalborg Universitetsforlag. Ph.d.-serien for Det Ingeniør- og Naturvidenskabelige Fakultet, Aalborg Universitet, 2018, ISBN 978-87-7210-134-7.

[13] A. Faaij R. Slade R. Mawhood M. Junginger S. de Jong R. Hoefnagels. "The feasibility of short-term production strategies for renewable jet fuels – a comprehensive techno-economic comparison," *Biofuels Bioproducts Biorefining*, vol. 9, pp. 778-800, 2015.

[14] W. Knoche. Chemical Reactions of CO_2. in C. Bauer, G. Gros H. Bartels (eds.) *Biophysical and Physiology of Carbon Dioxide*. Proceeding in Life Sciences. Springer, Berlin, Heidelberg, 1980. ISBN: 9783642675744.

[15] W. Knoche. , Chemical Reactions of CO_2 in Water. in C. Bauer, G. Gros H. Bartels (eds.) *Biophysical and Physiology of Carbon Dioxide*. Proceeding in Life Sciences. Springer, Berlin, Heidelberg, 1980. ISBN: 9783642675744.

[16] K. Aim M. Lísal W. R. Smith. "Analysis of Henry's Constant for Carbon Dioxide in Water via Monte Carlo Simulation," *Fluid Phase Equilibria*, vol. 226, pp. 161-172, 2004.

[17] R. L. Rowley M. Z. Southard. , Physical and Chemical Data. in MZ Southard DW Green (eds) *Perry's Chemical Engineers' Handbook, 9th Edition.* McGraw-Hill Education. ISBN:978-0-07-183408-7.

[18] *Maxwell-Bonnell-Calculator*. `http://pilodist.de/news/maxwell-bonnell-calculator/`. Accessed: 29.05.2019.

[19] Shailesh N. Shah Nikul K. Patel. , Biodiesel from Plant Oils. in Satinder Ahuja (eds.) *Food, Energy, and Water*. Elsevier, 2015. ISBN: 9780128002117.

[20] E. Weidner P. Ilieva A. Kilzer. "Measurement of solubility, viscosity, density and interfacial tension of the systems tristearin and CO2 and rapeseed oil and CO2," *The Journal of Supercritical Fluids*, vol. 117, pp. 40-49, 2016.

[21] C. R. de Souza Filho R. E. Correa Pabón. "Crude oil spectral signatures and empirical models to derive API gravity," *Fuel*, vol. 237, pp. 1119-1131, 2019.

[22] Esben Ravn. "Internship at Steeper Energy for Commissioning of a New State-of-the-Art HTL Product Separation and Demineralisation System, M.Sc. Project." Department of Energy, Aalborg University, Denmark, 8. Jan. 2019.

[23] M. Ben Isa S. J. Ashcroft. "Effect of Dissolved Gases on the Densities of Hydrocarbons," *Journal of Chemical Engineering Data*, vol. 45, pp. 1244-1248, 1997.

[24] *Shell Chemicals - Technical Datasheet - Methyl Ethyl Ketone*. `https://www.shell.com/business-customers/chemicals/our-products/solvents-chemical/ketones/_jcr_content/par/tabbedcontent/tab/textimage.stream/1459943761987/aa4a0ecc902a57b7ba182491ba379c14133dfab1/mek-s1213-global.pdf`. Accessed: 28.05.2019.

[25] Ian M. Smallwood. Handbook of Organic Solvent Properties, Arnold, Great Britain, ISBN: 9780340645784.

[26] W. Fei X. Gui Z. Tang. "Solubility of CO2 in Alcohols, Glycols, Ethers, and Ketones at High Pressures from (288.15 to 318.15) K," *Journal of Chemical Engineering Data*, vol. 56, pp. 2420-2429, 2011.

A Equilibrium Constants for the CO_2 in Water Reaction Mechanism

To assess how the equilibrium shifts as a function of temperature for the CO_2 in the water reaction mechanism, the Van't Hoff equation is used. The equation assumes that the heat of reaction is constant. The reaction mechanism is presented in Equation A.1 to A.3 and the Van't Hoff equation is presented in Equation A.4.

$$CO_2(aq) + H_2O \rightleftharpoons H_2CO_3 \tag{A.1}$$

$$H_2CO_3 \rightleftharpoons H^+ + HCO_3{}^- \tag{A.2}$$

$$HCO_3{}^- \rightleftharpoons H^+ + CO_3{}^{2-} \tag{A.3}$$

$$ln\left(\frac{K_{e2}}{K_{e1}}\right) = -\frac{\Delta H_r}{R_{univ}} \cdot \left(\frac{1}{T_2} - \frac{1}{T_1}\right) \tag{A.4}$$

Where:

- $K_{e1,e2}$ is the equilibrium constant at the given temperature, respectively [-].
- ΔH_r is the enthalpy of reaction for the given reaction ($\sum \Delta H_{f,products}$ - $\sum \Delta H_{f,reactants}$) [J/mol].
  - $\Delta H_{f,products}$ is the enthalpy of formation for the products [J/mol].
  - $\Delta H_{f,reactants}$ is the enthalpy of formation for the reactants [J/mol].
- R_{univ} is the universial gas constant, which is 8.314 J/(K · mol).
- $T_{1,2}$ is the temperature associated with the equlibrium constant, $K_{e1,e2}$, respectively [K].

The heat of formation is used to calculate the heat of reaction for each reaction. Reaction A.1 and A.2 are combined as only approximately 1 % of the CO_2(aq) is converted into H_2CO_3, and the Reaction A.1 do not contribute to the decrease in pH, as no H^+ is formed. The heat of formation for the compounds in the reaction mechanism are listed in Table A.1 at standard conditions (25 °C and 1 atm)

	H_2O(liq)	**CO_2(aq)**	**H_2CO_3(aq)**	**H^+(aq)**	**HCO_3^-(aq)**	**CO_3^{2-}(aq)**
ΔH_f° **[kJ/mol]**	-285.5	-419.3	-275.2	0	-689.9	-675.2

Table A.1: Enthalpy of formation for the compounds in the CO_2 reation mechanism at standard conditions.

By the Van't Hoff equation and the known equilibrium constants at standard condition, the equilibrium constants can be calculated for other temperatures. The equilibrium constant for the combined Reaction A.1 and A.2 is $4.45 \cdot 10^{-7}$ and the constant for Reaction A.3 is $4.69 \cdot 10^{-11}$ at standard conditions [5]. The equilibrium constants for 10 °C and 100 °C are presented in Table A.2.

	ΔH_r **[kJ/mol]**	**K_e(@25°C) [-] standard conditions**	**K_e(@10°C) [-]**	**K_e(@100°C) [-]**
Reaction A.1 and A.2	15.2	$4.45 \cdot 10^{-7}$	$3.99 \cdot 10^{-7}$	$4.70 \cdot 10^{-7}$
Reaction A.3	-400.1	$4.96 \cdot 10^{-11}$	$8.90 \cdot 10^{-10}$	$1.17 \cdot 10^{-11}$

Table A.2: Enthalpy of reaction and equilibrium constants.

By examine the enthalpy of reactions in Table A.2, the combined Reaction A.1 and A.2 is endothermic, as its enthalpy of reaction is positive. Reaction A.3 is exothermic, as its enthalpy of reaction is negative. The endothermic and exothermic behaviour of the reactions is also given in the equilibrium constants.

B Evaporation of MEK from Product Samples

The MEK concentrations vary within the product samples and feeds for the continuous experimental campaign. To compare product sample results from different feeds, it is important to know their MEK concentrations.

In the laboratories at Aalborg University, it is possible to evaporate five samples at a time, which would lower the spend time on these measurements. The five sample set-up is depicted in Figure B.1. This set-up could result in inaccurate MEK concentrations, as the surface area is increased when compared to a single sample set-up. A control sample is tested in the evaporator, which is Feed 4 in Table B.1. The measured MEK concentration for the control sample is 67.9 wt.%, and the actual value is 66.7 wt.%. The actual value is obtained by mixing the feed with a known oil phase mass and a known MEK mass. The difference between the actual and measured MEK concentration is 1.8 %. This value could be associated with the content of lights in the Hydrofaction™ oil, which has been measured to be 1.45 wt.%. Some of the lights have a boiling lower or similar to MEK, which is why they are evaporated off together with MEK. It is also possible that a small amount of water has been removed from the samples. Despite the small inaccuracies, the evaporation method is considered acceptable for the MEK evaporation of the product samples.

Figure B.1: Picture of the evaporator set-up for evaporating MEK from product samples.

The evaporator is a rotary vacuum evaporator. By decreasing the pressure, the evaporation temperature is reduced. The water bath, which is heating the samples is set to 60 °C. The pressure is slowly decreased to 150 mbar. It is expected that the temperature of the vaporous compounds of the product sample is cooled from the 60 °C to 40-50 °C before they reach the condenser. The atmospheric equivalent temperatures (AET) at 40-50 °C and 150 mbar are 78.5-89.5 °C [18]. The AET correspond well to the boiling point of MEK, which is 80 °C at ambient conditions [24].

The procedure for the MEK evaporation is:

1. An empty vial is weighed.
2. Approximately 20 g of product sample is poured into the vial, and the full vial is weighed.
3. Five full vials are connected to the rotary vacuum evaporator.
4. The evaporation duration is approximately 2 hours due to the slow decrease in pressure to 150 mbar.
5. When no vapour is observed in the condenser the evaporation is finished, and the vials are weighed again.

The MEK concentration of the product samples is calculated from the equation below.

$$MEK_{concentration} = \frac{Full_{vial} - Evaporated_{vial}}{Full_{vial} - Empty_{vial}}$$

Results from the evaporation of MEK for the product samples are presented in B.1. Note that some of the product samples have not been evaporated, due to their small sample size of 15-20 mL. Ash and water content of the product samples are also measured, and the amount of sample in the small samples are not enough to perform the MEK evaporations.

Sample #	Empty vial [g]	Full vial [g]	Evaporated vial [g]	Calc. MEK concentration [wt.%]
Feed 1	90.65	108.58	99.12	52.8
Feed 2	113.80	136.59	122.51	61.8
Feed 4	116.73	137.15	123.28	67.9
3	115.76	136.27	130.81	30.6
6	106.40	126.71	118.29	42.5
9	118.88	141.19	131.13	47.9
10	106.46	125.14	115.40	52.2
13	113.88	131.78	120.24	64.4
14	115.84	137.57	127.38	66.0

Table B.1: MEK evaporation data

C Solubility Calculations

Henry's law is used to estimate the solubility of CO_2 in the different liquid phases of the separation and demineralisation process. Henry's law states that the amount of gas dissolved in a solvent is proportional to the partial pressure of the gas with the proportional constant, Henry's constant. Henry's law is presented in Equation C.1.

$$c = \frac{P_i}{K_h} \tag{C.1}$$

Where:

- K_h is Henry's constant [Pa].
- P_i is the partial pressure of gas [Pa].
- c is the gas in liquid mole fraction [-].

The Henry's constant is dependent on the gas, solvent and temperature. The constants used in the report are derived from literature, and all presented constants are at 1 atm. Figure C.1 illustrates the Henry's constant for CO_2 in pure water and for CO_2 in a 5 N NaCl aqueous solution. Figure C.2 for CO_2 in MEK.

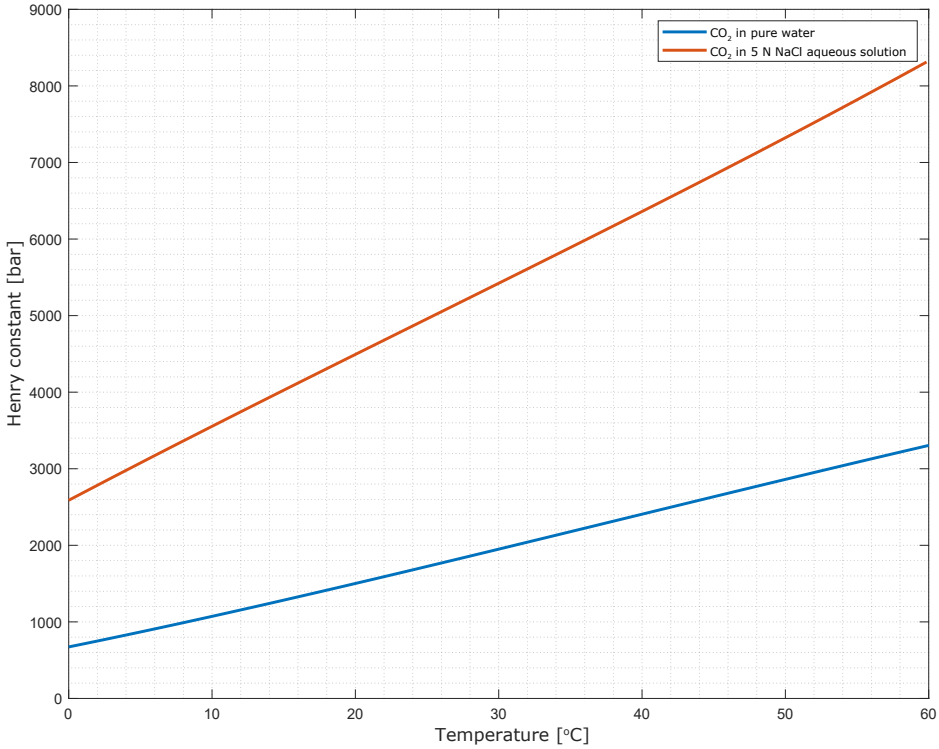

Figure C.1: Empirical curve fit from [16] based on a experimental study on Henry's constants of CO_2 in pure water and extrapolated Henry's constants for CO_2 in a 5 N NaCl solution from [8].

Figure C.1 illustrates a higher Henry's constant for CO_2 in an aqueous solution with a dissolved salt than for pure water.

The Henry's constant for CO_2 in MEK, when compared to CO_2 in pure water and an aqueous solution with dissolved salt, is between 25 and 90 times lower, based on the results in the Figures.

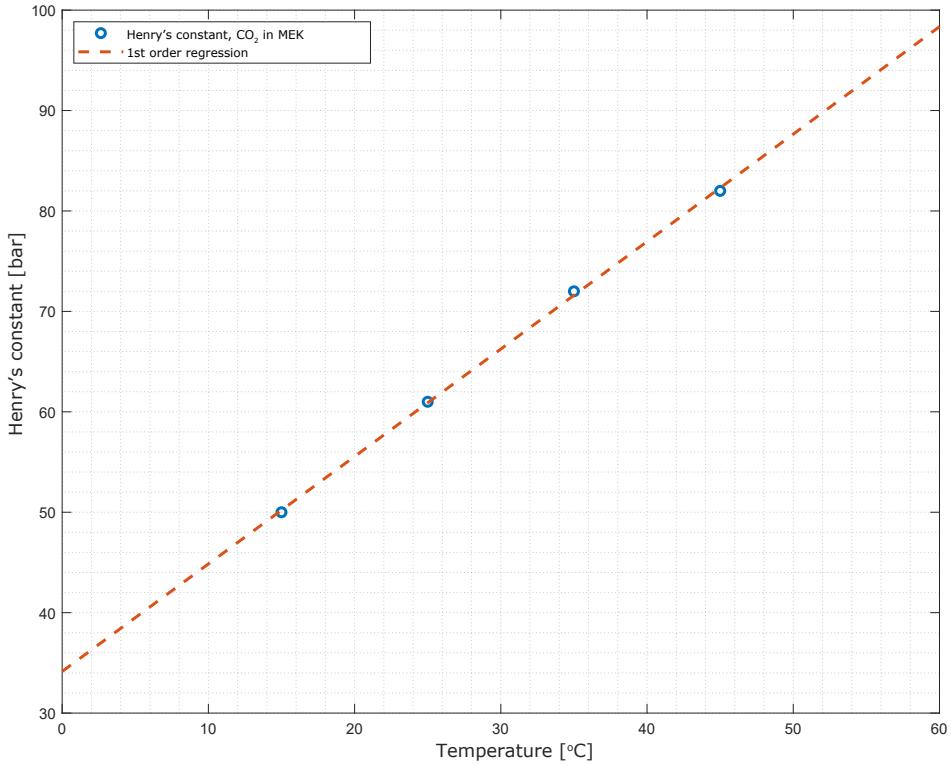

Figure C.2: Empirical Henry's constants for CO_2 in MEK from [26]. The 1st order regression is considered a suitable fit within the temperatures displayed in the figure.

D Solubility of CO_2 in Hydrofaction™ Oil

From the Henry's constants for MEK in Table 5.3 and the steady pressures in Table 5.2 the mass of CO_2 in MEK can be calculated by Henry's law in Equation 3.11.

$$
\begin{aligned}
Massfrac =& \frac{P_{steady}}{HenryConstant_{MEK}} \cdot \frac{MW_{CO_2}}{MW_{MEK}} \\
Massfrac_{BlankFeedCold} =& \frac{20.1bar}{54bar} \cdot \frac{44g/mol}{72.1g/mol} = 0.23g\mathrm{CO_2}/gMEK \\
Massfrac_{BlankFeedHOT} =& \frac{27bar}{90bar} \cdot \frac{44g/mol}{72.1g/mol} = 0.18g\mathrm{CO_2}/gMEK
\end{aligned}
$$

The calculated mass fractions reasonably match the mass fractions presented in Figure 3.3.

The MEK concentration used in the blank feed experiments is known and is 60 wt.%. The mass of feed, which is pumped into the vessel is 8.6 kg. Then the mass of MEK in the vessel is 5.2 kg. If the MEK in the vessel is saturated with CO_2 the mass of CO_2 in MEK would be:

$$
\begin{aligned}
Mass_{CO2} =& Massfrac \cdot Mass_{MEK} \\
Mass_{CO2,BlankFeedCold} =& 0.23g\mathrm{CO_2}/gMEK \cdot 5.2kg = 1.18kg\mathrm{CO_2} \\
Mass_{CO2,BlankFeedHOT} =& 0.18g\mathrm{CO_2}/gMEK \cdot 5.2kg = 0.95kg\mathrm{CO_2}
\end{aligned}
$$

Based on the volume of gas in vessel 2 from Table 5.2 and density calculations on CO_2 from the thermophysical property functions in EES® (at the steady temperature and pressure in Table 5.2), the amount of CO_2 dissolved in the feed is estimated. The calculations are based on a constant volume of the CO_2. However, to assess the sensitivity of the gas volume, it is increased and decreased by 10 % in the calculation.

- **Blank-Feed-Cold:** = 0.91 kg CO_2 in the feed.
  - **Sensitivity:** ($\pm$ 10 %) = 0.82 to 0.99 kgCO_2
- **Blank-Feed-Cold:** = 0.77 kg CO_2 in the feed.
  - **Sensitivity:** ($\pm$ 10 %) = 0.69 to 0.84 kgCO_2

From the above calculations, all CO_2 in the feed is dissolved in the MEK part of the feed. The MEK is not saturated based on its Henry's constants. 1.18 and 0.95 kg CO_2 can be dissolved in MEK and 0.91 and 0.77 kg CO_2 is dissolved in the feed for the cold and hot experiment, respectively. Based on the calculations, and if the Hydrofaction™ oil and MEK exist as two distinct phases in the feed, no CO_2 is dissolved in the oil. However, presumably the solubility of the oil/MEK mixture are different from their individual solubilities.